SEASONAL VARIATIONS OF PAVEMENT DEFLECTIONS IN TEXAS

by

Rudell Poehl
Engineering Research Associate

and

Frank H. Scrivner
Research Engineer

Research Report No. 136-1
Design and Evaluation of Flexible Pavements
Research Study 2-8-69-136

Sponsored by

The Texas Highway Department
In Cooperation with the
U. S. Department of Transportation
Federal Highway Administration

January, 1971

TEXAS TRANSPORTATION INSTITUTE
Texas A&M University
College Station, Texas

Preface

This is the first report issued under Research Study 2-8-69-136, Design and Evaluation of Flexible Pavements, being conducted at the Texas Transportation Institute as part of the cooperative research program with the Texas Highway Department and the Department of Transportation, Federal Highway Administration. The report gives the results of Phase 1, "Seasonal Strength Variations," now substantially complete.

The authors are grateful to Texas Highway Department personnel of Districts 4, 8, 19, 20 and 22 for their generous help in the selection of test sections and the installation of instrumentation. Thanks are also due Messrs. James L. Brown and Larry J. Buttler, Texas Highway Department Study Contact Representatives, for their assistance and support in the research, and Messrs. W. M. Moore and C. H. Michalak of the Institute, for their help in planning, data reduction and analysis.

The opinions, findings and conclusions expressed in this publication are those of the authors and not necessarily those of the Department of Transportation, Federal Highway Administration.

Abstract

Seasonal variations in the strength of flexible pavements are known to influence their service life, especially in the northern United States and Canada. Less is known regarding seasonal effects in a milder climate such as that of Texas. This study was undertaken in an attempt to determine where and when, in Texas, such variations exist, what their magnitudes are, and how they should be accounted for in the pavement design process.

Using deflections produced by a standard loading system (the Dynaflect) as an index to strength, periodic measurements were made over one year's time at 180 test points on flexible pavements located in five widely separated areas of the state.

The results indicated that seasonal changes in strength do exist in Texas, that above-average deflections usually occur in the spring and summer months, and that although the magnitude of the changes are generally smaller than those reported farther north, they are sufficiently great to warrant attention by the engineer using a deflection-based design system.

Summary

The new flexible pavement design system now on trial in several Texas Highway Department Districts relies upon deflection measurements made on existing highways for characterizing subgrade and other materials. If important seasonal variations in deflections occur in Texas it is important to the proper functioning of this design system to know the magnitude of these variations, and in particular to know when greater-than-average deflections are most likely to occur in a given locality.

In this context an attempt was made in this study to furnish some guide lines to users of the system, and to convey some general information regarding the variation of pavement deflections with both time and space. To this end, Dynaflect deflection data were gathered periodically from December, 1968, to November, 1969, at 180 test points evenly distributed between Districts 4, 8, 19, 20 and 22.

In each of the five districts six 1000-foot test sections were selected to cover a range of designs. Three test points, spaced at ten feet longitudinally, were marked in the outer wheel path near each end of each section. The periodic (approximately monthly) measurements at each test point yielded information regarding the variation of deflections with time alone. Since only a few days were required to make one set of measurements at all 180 points, there was also an opportunity to study the variation of deflections with distance or location.

Some of the findings with regard to variations with time and space are summarized below:

1. A sine curve, with a period of one year, was found to be a suitable mathematical model of the variation with time of the deflection measured at a test point.
2. With respect to deflections occurring at the two ends of a 1000-foot, apparently uniform test section, it may be said that the odds are about two to one that
   (1) the annual means of the deflections at the two ends will differ significantly, and
   (2) the annual changes in deflection at the two ends will differ significantly.
3. In a mile or more of pavement of the same design, the odds are high that the variation in deflections measured on the same day at intervals of say, 1000 feet, will exceed the annual variation at any one of the measuring points. Thus it appears that seasonal changes in the deflection of flexible pavements in Texas are usually less important than the random changes in the pavement-subgrade system that occur in distances that - from the designer's viewpoint - are relatively short (say one mile).
4. Within a district, the annual percentage change in deflection may be expected to differ significantly from one highway to the next.
5. The annual percentage change in deflection was usually greater in the eastern (wet) part of Texas, than in the western (dry) area.
6. Deflections measured in the spring at a point in either of the two eastern districts tended to exceed the annual mean at that point, while in the three western districts deflections tended

to be highest in the summer. There was no discernible trend in the time of occurrence of high deflections between northern and southern districts having approximately the same annual rainfall. It was concluded that annual rainfall is related to the timing of the annual maximum deflection at a point in Texas, while the mean annual temperature is not. (This finding, however, is not intended to rule out the possibility that in some years, on some pavements, sudden, brief and extreme increases in deflections will occur in the northern portions of the state, especially in the Panhandle, during the thaw following a protracted period of freezing weather.)

7. Although variations of deflection with time were found to be generally smaller than variations encountered in relatively short distances (say one mile), it still appears advisable for the engineer using the current version of the deflection-based pavement design system to attempt to measure the deflections of existing highways during the three-month period when deflections in his locality are most likely to exceed their annual mean. (A method for estimating the proper time for making the measurements is described in Chapter 6.)
8. An alternate and, in the long run, perhaps a more practical procedure than that recommended in the preceding paragraph, would be to modify the current version of the flexible pavement design system computer program to receive a random (unexplained) variable to represent seasonal variations in deflections. The work of modifying the program is considered

to be beyond the scope of this research. Some of the necessary basic data have been collected in this study, are stored on IBM cards at Texas Transportation Institute, and are readily available when required.

Implementation Statement

The report is directed mainly to those Texas Highway Department engineers who are using (presently on a trial basis) the flexible pavement design system developed in Research Studies 2-8-62-32 and 2-8-69-123, and to those engineers of the Department who share with their research agencies the responsibility of up-dating the system as new data become available. The data presented support a recommendation that the deflections of existing highways required in the use of the current version of the system be measured in the three-month period during which deflections are most likely to exceed their annual average value. A means for roughly estimating this period for any given location in Texas is given in Chapter 6 of the report.

The data also suggest that an investigation be undertaken to determine the desirability of introducing a random (unexplained) variable into the system to account for seasonal variations in deflections.

Table of Contents

Table of Contents (continued)

List of Figures

List of Figures (continued)

List of Tables

List of Tables (continued)

1. Introduction

The Texas Highway Department is now engaged in implementing, on a trial basis, a flexible pavement design system (1) containing an important subsystem that directly relates the probable service life of a proposed design to its predicted deflection under a 9000-pound wheel load. The inputs to the subsystem include deflection measurements made on existing highways in the general area where the proposed design is to be constructed. These measurements strongly influence the predictions of the service life of the design. Thus, if significant seasonal variations in pavement deflections occur regularly in Texas, it is of considerable importance to know where they occur, when they occur, and how large they are.

This report attempts to answer the questions . . . when? . . . where? . . . how large? . . . by presenting the results of a series of statistical analyses of deflection data gathered periodically over a one-year period at 180 test points in five Texas Highway Department Districts. The answers are seldom clear cut - they must be given in probabilistic terms.

For instance, based on data taken in 1969, one can say that if a deflection is measured between the middle of June and the middle of September at a point selected at random in the outer wheel path of a highway in District 4, the chances are about 8 in 10 that the deflection measured will be greater than the annual average deflection at that point. The answer to "when?" is a specified three-month period; to "where?" it is ". . . a point selected at random . . . in District 4";

to "how large?" it is "greater than the annual average deflection at that point."

Perhaps none of these answers - which are typical of several given in Chapters 4, 5 and 6 of the report - will satisfy the reader looking for precise guidance in the use of the new flexible pavement design system. To him the authors offer their apologies, but add that the report may serve at least to emphasize the need for considering, in any design system, the stochastic nature of the variables with which we must deal.

2. Experiment Design

The selection of geographical areas for locating test sections was based on the assumption that variables most likely to be associated with seasonal variations in stiffness are precipitation rate and ambient temperature. To permit an evaluation of the effect of these variables and possible freeze-thaw action, six test sections were selected in each of the five districts indicated in Figure 1. A factorial involving Districts 8, 19, 20 and 22 allows an evaluation of the effect of different precipitation rates between districts of similar temperatures, and the effect of different temperatures between districts of similar precipitation rates. Sections were selected in District 4 because it is the Texas area most likely to be affected by freeze-thaw action.

The six test sections in each district were selected to provide a range of deflections representative of the highways in that district. The selections were made, with the aid of the Dynaflect, from locations suggested by district personnel. Table 1 describes the locations of the 30 test sections selected. An attempt to secure uniformity of structure (including the foundation) was made in choosing each 1000-foot section.

Six test points, three near each end of each section, were permanently marked in the outer wheel path so that the deflection tests could be made at the same points on successive visits by the testing crew. The layout of a typical test section, with its two subsections, is shown in Figure 2. The indicated configuration of test points permits the detection of statistically significant differences in deflection that may occur within a one-thousand foot section of an apparently uniform pavement and subgrade.

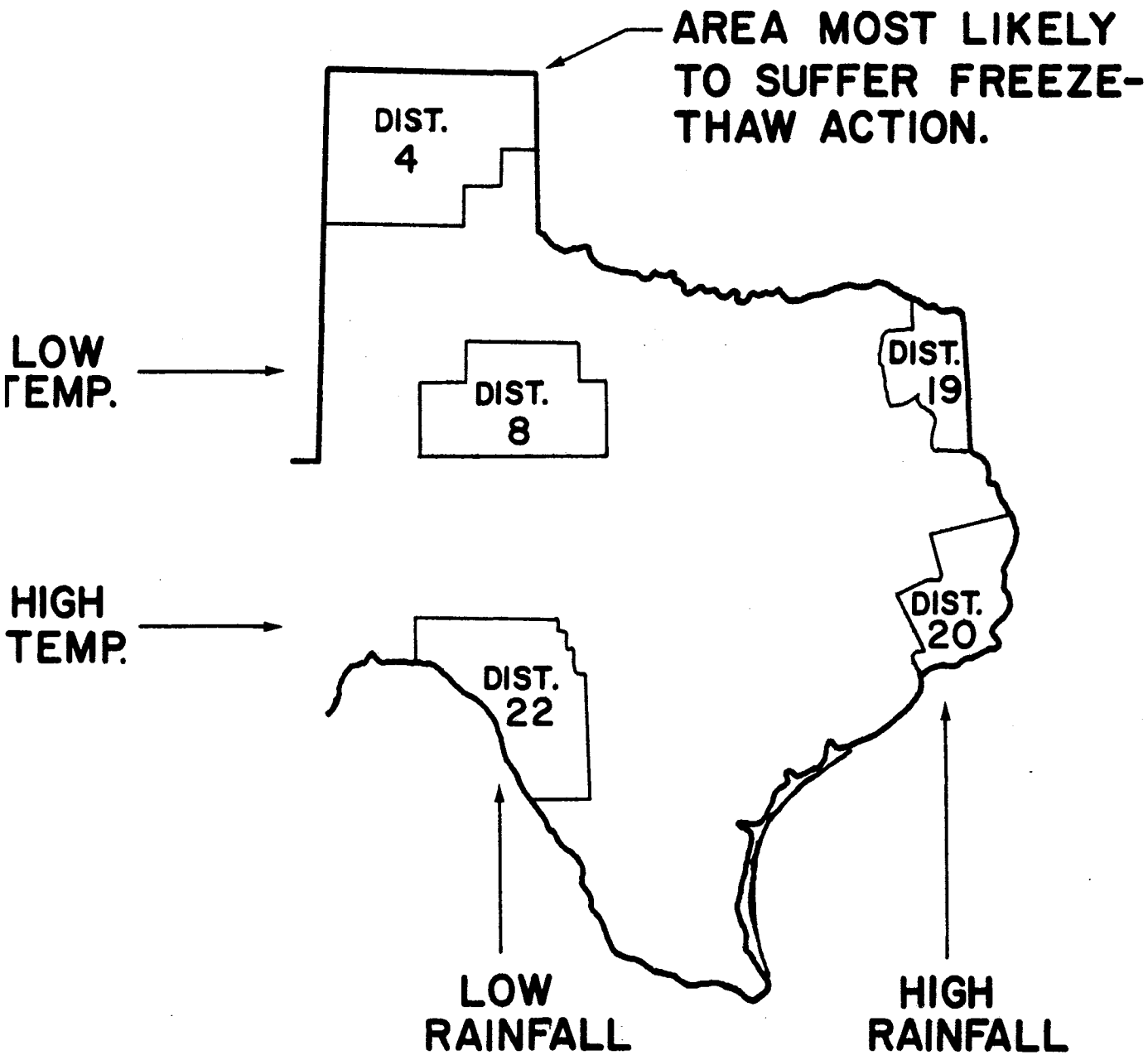

FIGURE 1 - Areas selected for the study of seasonal variations in deflection.

Table 1: Location of Test Sections

District	Sec. No.	Highway	County	Location	Traffic Direction
4	1	US 60	Randall	2 mi W US 87	West
4	2	US 66	Potter	4 mi E Bushland	East
4	3	FM 1061	Potter	1 mi NW US 66	Southeast
4	4	SH 152	Moore	3 mi E Dumas	East
4	5	SH 152	Hutchinson	1 mi E FM 1913	East
4	6	US 287	Armstrong	1 mi E Goodnight	East
8	1	FM 57	Fisher	1 mi NE McCaulley	Southwest
8	2	SH 70	Nolan	0.5 mi N Blackwell	North
8	3	US 84	Nolan	2 mi NW Roscoe	Northwest
8	4	IH 20	Nolan	2 mi W Roscoe	East
8	5	SH 208	Mitchell	11 mi S Colorado City	South
8	6	IH 20	Mitchell	3 mi W Westbrook	West
19	1	SH 77	Cass	0.2 mi E FM 251	West
19	2	US 59	Bowie	0.5 mi N Sulphur R.	North
19	3	FM 2148	Bowie	2 mi N US 67	North
19	4	FM 2240	Bowie	0.2 mi E FM 559	East
19	5	US 259	Bowie	2 mi N US 82	North
19	6	FM 2790	Bowie	1 mi W US 259	West
20	1	FM 418	Hardin	0.5 mi W FM 92	West
20	2	SH 327	Hardin	4 mi W Silsbee	East
20	3	US 69, 96 & 287	Jefferson	2 mi N SH 105	South
20	4	FM 365	Jefferson	1 mi E FM 1406	West
20	5	FM 365	Jefferson	8 mi E Fannett	West
20	6	SH 73	Jefferson	7 mi W US 69, 96 & 287	West
22	1	US 377	Edwards	5 mi NE FM 2523	Northeast
22	2	US 277 & 377	Val Verde	0.5 mi N US 90	North
22	3	FM 3008	Kinney	2 mi N US 90	South
22	4	FM 2369	Uvalde	2 mi N US 90	South
22	5	SH 57	Zavala	2 mi W La Pryor	West
22	6	SH 57	Maverick	9 mi NE US 277	Southwest

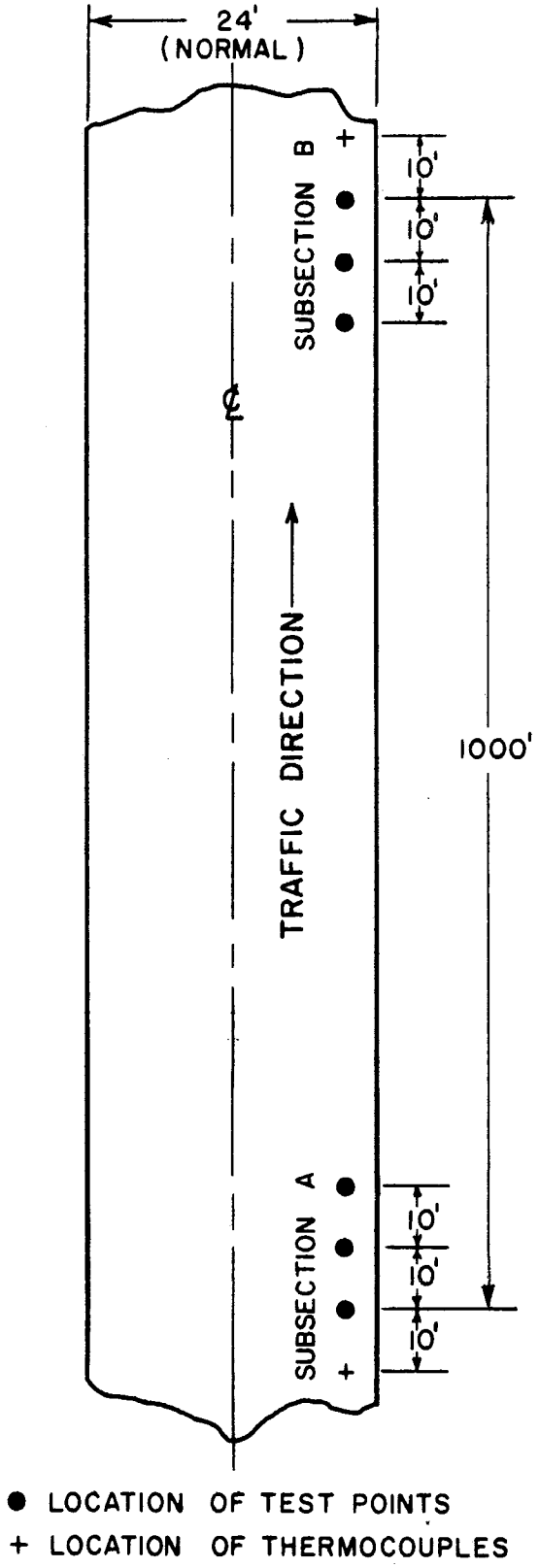

FIGURE 2 - Layout of test sections. There were six per district, thirty in all.

The structural design of each subsection, shown in Table 2, was determined from a hole drilled for installation of thermocouples just outside the test section limit. The mean annual deflection of each subsection shown in this table is the value predicted by a mathematical model (a sine curve) fitted to deflection data measured at intervals of about one month on the subsection for a period of one year. The mean deflection predicted by the model differed only slightly from the mean of the measured data. The model and the measured deflections are discussed in detail in Chapter 4.

Installations of thermocouples, sketched in Figure 3, were made to determine which areas of the state, if any, experienced appreciable frost penetration during the one-year period of observation. Thermocouples were installed in each subsection at depths ranging to 3 feet. The individual thermocouple spacing is shown in the sketch. A junction box was placed in the shoulder opposite each installation. The Texas Highway Department furnished personnel and equipment to drill holes for the installations.

Table 2: Nominal Design and Estimated Mean Deflection of Each Test Section

Dist No	Sec No	Subsec Code	Estimated Mean Defl (mils)	Thickness (Inches)			Material Type			
				Surface	Base	Subbase	Surface*	Base	Subbase	Subgrade
4	1	A	1.15	1.5	14	---	A.C.	Caliche	-------	Silty Clay
4	1	B	1.35	1.5	14.5	---	A.C.	Caliche	-------	Silty Clay
4	2	A	1.67	3	14.5	---	A.C.	Caliche	-------	Silty Clay
4	2	B	1.64	3	14.5	---	A.C.	Caliche	-------	Silty Clay
4	3	A	0.71	1	14.5	---	S.T.	Caliche	-------	Clay Silt & Fine Sand (Some Caliche)
4	3	B	0.72	1	12.5	---	S.T.	Caliche	-------	Clay Silt & Fine Sand (Some Caliche)
4	4	A	1.43	1	6	10***	S.T.	Gravel	Caliche	Silty Clay
4	4	B	1.63	1.2	7	9.8***	S.T.	Gravel	Caliche	Silty Clay
4	5	A	1.07	1	9	---	S.T.	Caliche	-------	Clay Silt & Sand
4	5	B	1.05	1	8.2	---	S.T.	Caliche	-------	Clay Silt & Sand
4	6	A	0.68	4	13	---	A.C.	Caliche	-------	Silty Sandy Clay
4	6	B	1.08	4	14.5	---	A.C.	Caliche	-------	Silty Sandy Clay
8	1	A	1.88	0.8	6.2	---	S.T.	Sandy Gravel	-------	Sandy Clay over Clay
8	1	B	2.12	0.8	6.5	---	S.T.	Sandy Gravel	-------	Sandy Clay over Clay
8	2	A	1.10	0.5	8.5	---	S.T.	Cr. Limestone	-------	Sandy Clay
8	2	B	1.10	0.5	8.5	---	S.T.	Cr. Limestone	-------	Sandy Clay
8	3	A	0.61	1.2	8	10.2	A.C.	Cr. Limestone	Caliche	Clay
8	3	B	0.56	1.2	8	12	A.C.	Cr. Limestone	Caliche	Clay
8	4	A	0.28	2.8	19.5	---	A.C.	Cr. Limestone	-------	Clay
8	4	B	0.35	3.2	18	---	A.C.	Cr. Limestone	-------	Clay
8	5	A	1.36	1	5.5	---	S.T.	Caliche Gravel	-------	Sandy Soil
8	5	B	1.52	1.2	5	---	S.T.	Caliche Gravel	-------	Sandy Soil
8	6	A	1.21	6	10	---	A.C.	Caliche Gravel	-------	Clay
8	6	B	1.21	6.2	12.5	---	A.C.	Caliche Gravel	-------	Clay
19	1	A	0.71	2	9.5	12**	A.C.	Iron Ore	Sand	Iron Ore Gravel
19	1	B	0.45	2**	10**	12**	A.C.	Iron Ore	Sand	Iron Ore Gravel

Table 2 continued: Nominal Design and Estimated Mean Deflection of Each Test Section.

Dist No	Sec No	Subsec Code	Estimated Mean Defl (mils)	Thickness (Inches)			Material Type			
				Surface	Base	Subbase	Surface*	Base	Subbase	Subgrade
19	2	A	1.27	2	10	12**	A.C.	Cem. Treat. Iron Ore	Sand	Clay
19	2	B	1.08	2	10	12**	A.C.	Cem. Treat. Iron Ore	Sand	Clay
19	3	A	1.13	0.5	6	20	S.T.	Iron Ore	Sand	Clay
19	3	B	1.09	0.5	5	21	S.T.	Iron Ore	Sand	Clay
19	4	A	1.59	0.9	1	20	S.T.	Iron Ore Gravel	Silty Sand	Sandy Clay
19	4	B	1.09	0.9	2.1	22	S.T.	Iron Ore Gravel	Silty Sand	Sandy Clay
19	5	A	0.85	2.2	8	13	A.C.	Cr. Limestone	Sand	Clay
19	5	B	0.75	2.2	10	12	A.C.	Cr. Limestone	Sand	Clay
19	6	A	1.15	0.5	8	24 est	S.T.	Cem. Treat. Sand	Sand	Clay
19	6	B	1.06	0.5	8	24 est	S.T.	Cem. Treat. Sand	Sand	Clay
20	1	A	0.43	0.8	7.2	6	S.T.	Sand Shell	Lime Treat. Sand	Sandy Loam
20	1	B	0.67	0.8	7.2	7.5	S.T.	Sand Shell	Lime Treat. Sand	Sandy Clay
20	2	A	1.04	2	4.8	3.5	A.C.	Sand Shell	Iron Ore & Shell	Sand
20	2	B	1.02	2	4.8	4	A.C.	Sand Shell	Iron Ore & Shell	Sand
20	3	A	1.24	3.5	11	7	A.C.	Sand Shell	Sand	Clay
20	3	B	1.17	3.5	14.5	4	A.C.	Sand Shell	Sand	Clay
20	4	A	2.58	0.8	8.2	4.5	S.T.	Sand Shell	Sand	Clay
20	4	B	2.00	1	8	6.5	S.T.	Sand Shell	Sand	Clay
20	5	A	1.54	0.8	7.2	9	S.T.	Sand Shell	Sand	Sandy Silty Clay
20	5	B	1.81	0.5	10	13.5	S.T.	Sand Shell	Sand	Sandy Silty Clay
20	6	A	2.35	4	9.5	4	A.C.	Sand Shell	Sand	Silty Clay
20	6	B	1.88	4	9.5	9	A.C.	Sand Shell	Sand	Silty Clay
22	1	A	0.65	0.5	5.5	---	S.T.	Cr. Limestone	-------	Clay (18") over Soft Limestone with Rock
22	1	B	0.49	0.5	6.5	---	S.T.	Cr. Limestone	-------	Clay (2") over Soft Limestone with Rock
22	2	A	0.30	1.5	12	---	L.R.A.	Cr. Limestone	-------	Clayey Caliche & Soft Limestone
22	2	B	0.32	1.5	12.5	---	L.R.A.	Cr. Limestone	-------	Clayey Caliche & Soft Limestone

Table 2 continued: Nominal Design and Estimated Mean Deflection of Each Test Section

Dist No	Sec No	Subsec Code	Estimated Mean Defl (mils)	Thickness (Inches)			Material Type			
				Surface	Base	Subbase	Surface*	Base	Subbase	Subgrade
22	3	A	1.40	0.5	9.5	---	S.T.	Caliche & Limestone	-------	Silty Clay (9") over Caliche & Soft Limestone
22	3	B	0.97	0.5	9.5	---	S.T.	Caliche & Limestone	-------	Silty Clay (5") over Caliche & Soft Limestone
22	4	A	2.42	1	4.5	---	S.T.	Caliche & Gravel	-------	Clay
22	4	B	3.02	1	5	---	S.T.	Caliche & Gravel	-------	Clay
22	5	A	0.97	1.5	11.5	---	L.R.A.	Caliche & Flint Gravel	-------	Clay over Silty Clay
22	5	B	1.23	1.5	11.5	---	L.R.A.	Caliche & Flint Gravel	-------	Clay over Silty Clay
22	6	A	2.61	0.8	6	---	S.T.	Caliche & Gravel	-------	Clay
22	6	B	1.53	0.8	4.8	19.5	S.T.	Caliche & Gravel	Lime Stab. Subg.	Sandy Silty Clay

*Seal coats have been applied to some if not all of these pavements.
**These thicknesses estimated from construction plans.
***These thicknesses include approximately 1" surface treatment of old highway.

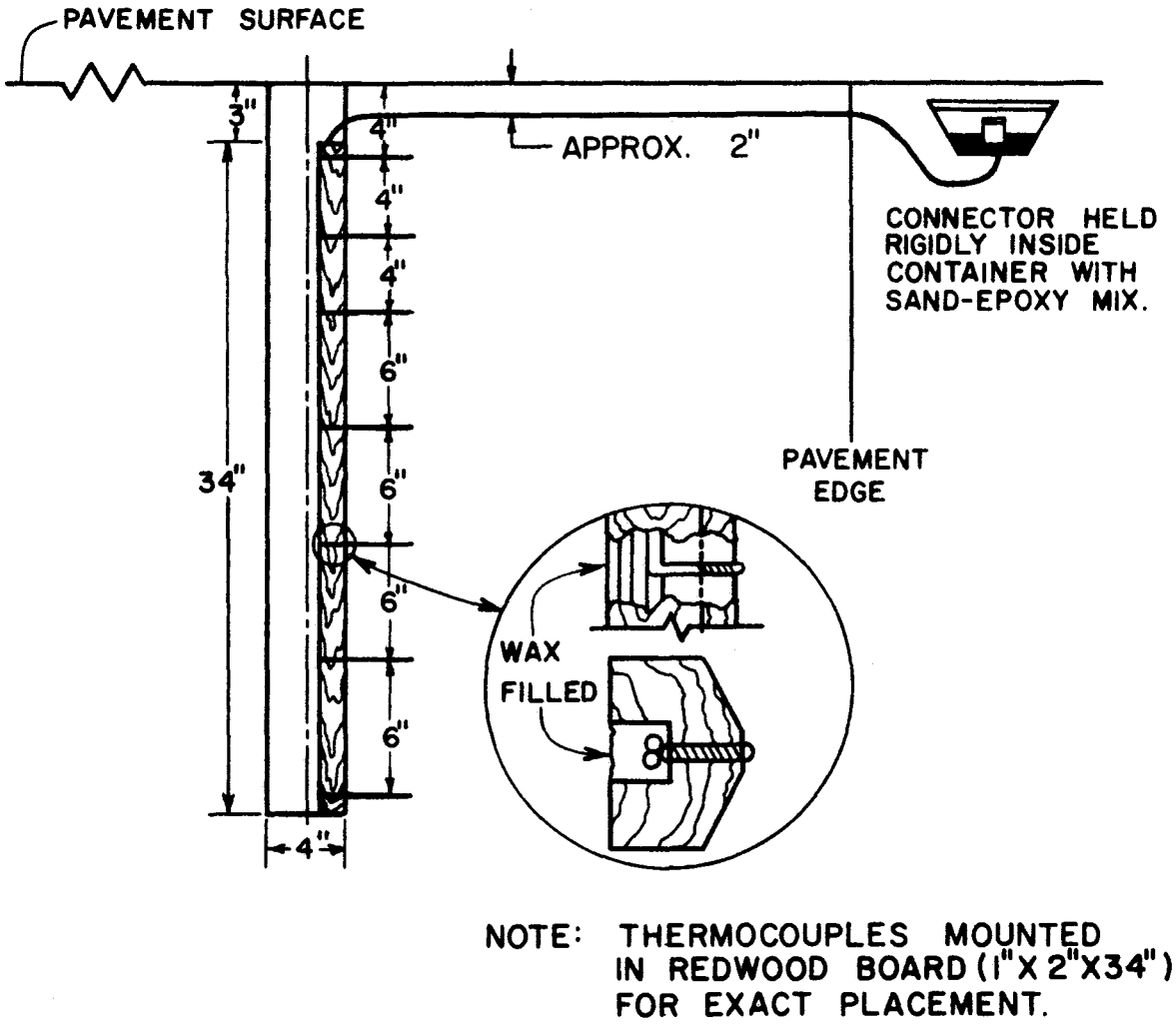

FIGURE 3 - Typical thermocouple installation. There were two per section, sixty in all.

3. Testing Program

The Dynaflect, an instrument mounted on a small two-wheel trailer (Figure 4) towed behind a passenger car, was used for loading the pavement and measuring the resulting deflections. For testing, a pair of steel load wheels are lowered to the pavement, lifting the travel wheels and transmitting to the pavement an oscillating load generated by eccentric weights rotating eight revolutions per second (Figure 5). A detailed description of the Dynaflect has been reported prior to this study (2). The procedure used in calibrating and operating the Dynaflect is given in Appendix A.

A Leeds and Northrup potentiometer with direct temperature readout was used in conjunction with the thermocouples for reading ground temperatures. The system was calibrated and the thermocouples read from inside a passenger car (Figure 6). The measurement procedure is given in Appendix A; the data are discussed in Appendix B.

A two-man testing crew from Texas Transportation Institute gathered all dynaflect and ground temperature data on the test sections. Flagmen were supplied by the Texas Highway Department wherever protection from traffic was required. Eleven visits were made to each test section during the test period from December, 1968, through November, 1969. During each visit, deflection data on each of the six test points of a section were obtained at five positions relative to the load wheels (Figure 7). Also observed on each visit were the air temperature, measured by thermometer, and ground temperatures indicated by each of the two sets of thermocouples located at opposite ends of the section.

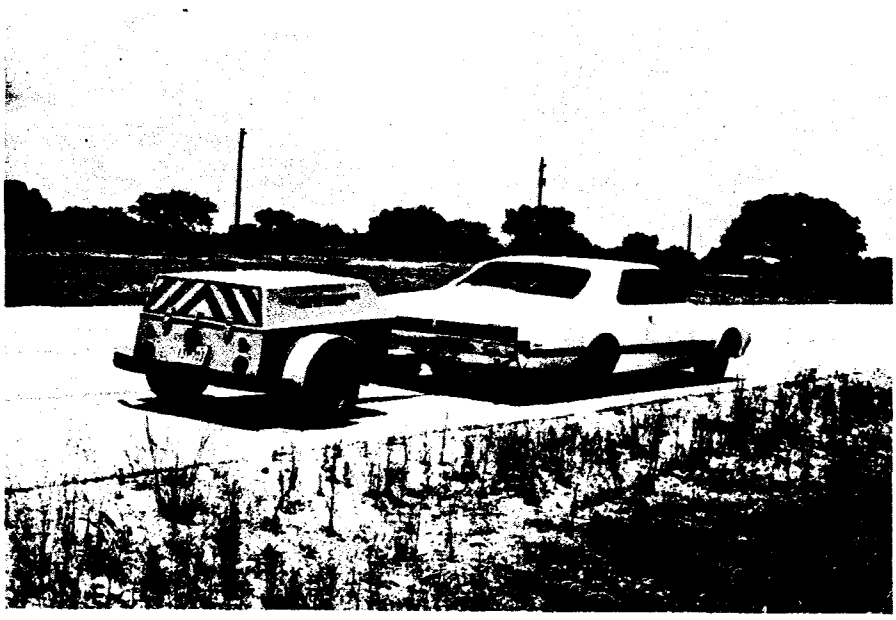

FIGURE 4 - Dynaflect ready for travel.

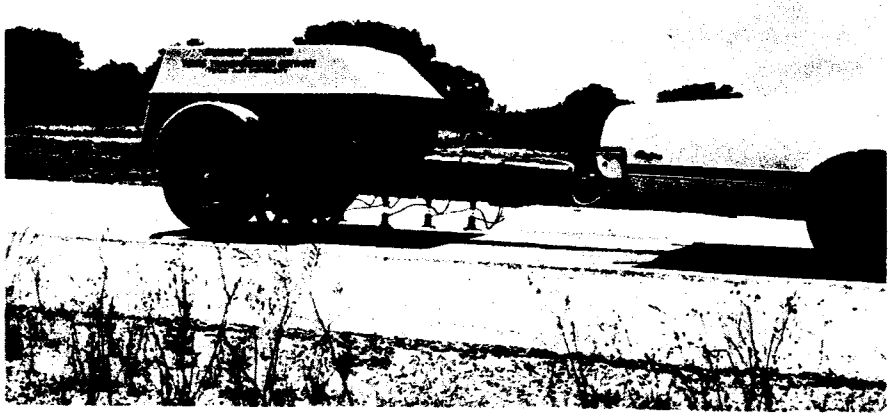

FIGURE 5 - Dynaflect supported on steel load wheels. Geophones, shown suspended from trailer tongue, are lowered to pavement prior to testing.

FIGURE 6 - Technician reading thermocouples. Geophones were also read from inside vehicle.

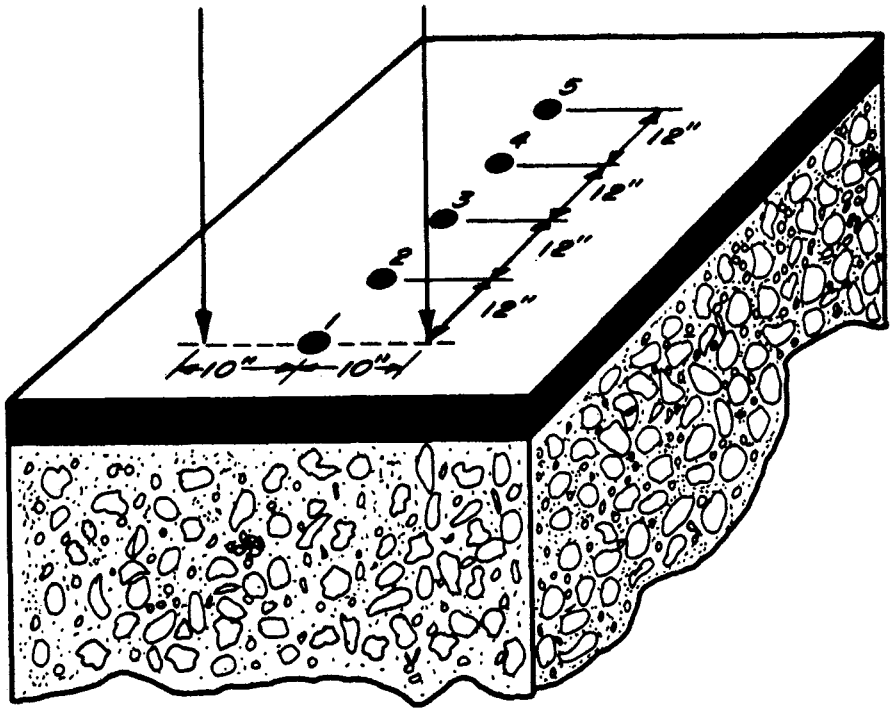

FIGURE 7 - Relative positions of Dynaflect load wheels (arrows) and geophones (numbered points). The reading at point 1 (W_1) was used in most of the analyses.

One visit to all test sections required approximately eight days. The dates of the eleven visits are listed below.

Visit	Inclusive Dates
1	Dec. 9-16, 1968
2	Jan. 21-27, 1969
3	Feb. 18-25, 1969
4	Mar. 24-31, 1969
5	Apr. 22-30, 1969
6	Jun. 2-9, 1969
7	Jun. 30-Jul. 8, 1969
8	Aug. 18-25, 1969
9	Sep. 22-30, 1969
10	Oct. 20-27, 1969
11	Nov. 18-25, 1969

4. Analysis of Deflection Data

Although deflections were measured at five positions relative to the load wheels at each test point during each visit, it was felt that seasonal variations could be detected from an examination of the deflection, W_1, measured directly between the load wheels. Hereafter the term "deflection" will mean the deflection, W_1, unless otherwise stated. This deflection, averaged for each subsection for each visit, is given in Table 3. Each entry in the table is the mean of three deflections measured in the outer wheel path within a distance of twenty feet (see Figure 2). Table 4 shows the estimated mean annual deflection for each district, together with the highest and lowest deflections observed.

4.1 Preliminary Studies of Deflection Data: Plots of deflection versus time for each subsection, like the one shown in Figure 8, suggested a seasonal trend. As the first step in an investigation of this possibility, an analysis of variance was made to determine whether the average maximum and average minimum deflection observed on each subsection during the test period were significantly different when compared to the variation within subsections. A significant difference was found, at the 10% level for 52 of the 60 subsections (Table 5). Five of the eight comparisons found not to be significantly different involved subsections located in District 22.

The Texas section that exhibited the greatest seasonal variation of deflections during this study is compared in Figure 9 to a section near Rochester, Minnesota, that was subjected to severe freeze-thaw action in 1966-67 (3).

District	Subsection	Visit Number										
		1	2	3	4	5	6	7	8	9	10	11
4	1A	1.07	1.10	1.16	1.03	1.19	1.13	1.21	1.21	1.16	1.23	1.16
	1B	1.26	1.23	1.24	1.21	1.42	1.40	1.42	1.39	1.41	1.51	1.29
	2A	1.53	1.58	1.59	1.57	1.71	1.73	1.90	1.75	1.65	1.63	1.64
	2B	1.47	1.56	1.55	1.54	1.70	1.70	1.82	1.75	1.62	1.62	1.58
	3A	0.73	0.72	0.72	0.67	0.70	0.69	0.67	0.74	0.73	0.77	0.70
	3B	0.72	0.69	0.70	0.65	0.69	0.69	0.70	0.81	0.77	0.82	0.70
	4A	1.36	1.26	1.25	1.34	1.52	1.59	1.55	1.56	1.42	1.36	1.37
	4B	1.53	1.44	1.41	1.51	1.64	1.84	1.81	1.79	1.67	1.61	1.58
	5A	1.00	0.98	0.96	1.00	1.09	1.13	1.14	1.16	1.12	1.10	1.03
	5B	0.99	0.96	0.96	0.98	1.04	1.10	1.12	1.17	1.09	1.07	1.03
	6A	0.65	0.63	0.67	0.67	0.71	0.72	0.70	0.74	0.70	0.63	0.63
	6B	0.91	0.91	0.95	1.01	1.16	1.23	1.20	1.29	1.21	0.93	0.95
8	1A	1.75	1.75	1.78	1.77	2.18	1.82	2.08	1.99	1.80	1.82	1.79
	1B	1.98	1.95	1.97	1.95	2.43	2.11	2.49	2.19	2.11	1.97	2.00
	2A	1.03	1.05	1.05	1.05	1.11	1.11	1.17	1.28	1.12	1.08	1.02
	2B	1.06	1.04	1.02	1.02	1.11	1.05	1.14	1.21	1.17	1.15	1.10
	3A	0.62	0.62	0.62	0.58	0.62	0.61	0.65	0.58	0.62	0.63	0.61
	3B	0.55	0.55	0.55	0.53	0.54	0.54	0.59	0.60	0.56	0.57	0.55
	4A	0.27	0.28	0.27	0.27	0.28	0.28	0.29	0.29	0.28	0.28	0.28
	4B	0.33	0.34	0.33	0.33	0.36	0.35	0.36	0.38	0.37	0.37	0.36
	5A	1.47	1.42	1.37	1.24	1.26	1.30	1.30	1.36	1.45	1.50	1.39
	5B	1.51	1.44	1.35	1.42	1.47	1.48	1.53	1.71	1.70	1.59	1.44
	6A	1.05	1.08	0.97	1.12	1.26	1.40	1.41	1.51	1.30	1.02	0.99
	6B	1.03	1.09	0.96	1.13	1.28	1.42	1.44	1.52	1.30	1.02	0.97

Table 3 continued: Mean Deflection ($\bar{W}_1$) of Each Subsection on Each Visit

District	Subsection	Visit Number 1	2	3	4	5	6	7	8	9	10	11
19	1A	0.71	0.67	0.74	0.73	0.79	0.75	0.73	0.66	0.68	0.68	0.66
	1B	0.46	0.47	0.47	0.46	0.47	0.45	0.43	0.40	0.43	0.45	0.46
	2A	1.21	1.11	1.24	1.27	1.36	1.39	1.35	1.26	1.28	1.22	1.17
	2B	1.00	0.94	1.02	1.05	1.19	1.16	1.15	1.14	1.14	1.05	1.00
	3A	1.15	1.07	1.18	1.19	1.26	1.22	1.11	1.08	1.06	1.02	1.01
	3B	1.12	1.05	1.12	1.10	1.19	1.19	1.06	1.07	1.06	1.00	1.00
	4A	1.85	1.67	2.19	1.94	1.84	1.72	1.49	1.24	1.24	1.16	1.21
	4B	1.42	1.21	1.50	1.32	1.22	1.15	0.88	0.81	0.78	0.76	1.07
	5A	0.87	0.86	0.96	0.84	0.86	0.83	0.79	0.77	0.81	0.85	0.89
	5B	0.79	0.78	0.92	0.87	0.84	0.78	0.68	0.59	0.66	0.68	0.72
	6A	1.11	1.10	1.23	1.15	1.20	1.23	1.26	1.10	1.14	1.04	1.06
	6B	1.09	1.07	1.15	1.03	1.02	1.03	1.07	1.01	1.04	1.12	1.03
20	1A	0.40	0.49	0.52	0.52	0.49	0.48	0.41	0.38	0.36	0.37	0.34
	1B	0.64	0.73	0.74	0.71	0.72	0.71	0.66	0.64	0.62	0.61	0.58
	2A	0.96	1.19	1.30	1.28	1.22	1.18	0.97	0.87	0.81	0.78	0.87
	2B	0.95	1.02	1.05	1.11	1.12	1.15	1.05	0.95	0.94	0.90	0.88
	3A	1.04	1.13	1.14	1.22	1.21	1.35	1.45	1.29	1.26	1.22	1.05
	3B	1.05	1.14	1.13	1.11	1.23	1.24	1.25	1.20	1.24	1.17	1.05
	4A	2.09	2.54	2.79	2.49	2.87	2.89	2.69	3.02	2.55	2.26	1.92
	4B	1.70	1.91	2.05	1.93	2.21	2.23	2.16	2.18	1.95	1.82	1.67
	5A	1.43	1.55	1.62	1.57	1.56	1.65	1.51	1.63	1.51	1.48	1.42
	5B	1.77	1.90	1.98	1.96	1.97	1.83	1.70	1.84	1.71	1.70	1.55
	6A	2.32	2.53	2.62	2.42	2.56	2.51	2.21	2.24	2.32	2.14	2.00

Table 3 continued: Mean Deflection ($\bar{W}_1$) of Each Subsection on Each Visit

District	Subsection	Visit Number 1	2	3	4	5	6	7	8	9	10	11
22	1A	0.63	0.64	0.61	0.61	0.67	0.75	0.72	0.67	0.60	0.63	0.58
	1B	0.50	0.49	0.49	0.48	0.47	0.52	0.47	0.49	0.48	0.52	0.47
	2A	0.30	0.30	0.29	0.29	0.30	0.31	0.30	0.32	0.31	0.30	0.28
	2B	0.26	0.29	0.27	0.29	0.31	0.33	0.32	0.35	0.35	0.36	0.33
	3A	1.41	1.45	1.39	1.29	1.41	1.47	1.41	1.53	1.37	1.34	1.29
	3B	0.98	1.02	0.96	0.95	0.97	1.00	0.93	1.01	0.96	0.94	0.91
	4A	2.42	2.50	2.39	2.32	2.43	2.25	2.41	2.54	2.47	2.50	2.43
	4B	3.23	3.08	3.27	3.13	2.98	2.85	2.73	3.10	3.19	3.01	2.73
	5A	0.92	0.91	0.92	0.93	0.99	0.99	0.99	1.02	1.03	0.97	0.92
	5B	1.11	1.20	1.24	1.18	1.26	1.23	1.29	1.29	1.26	1.24	1.23
	6A	2.51	2.49	2.54	2.33	2.49	2.49	2.70	2.85	2.91	2.70	2.61
	6B	1.42	1.50	1.52	1.49	1.65	1.60	1.65	1.65	1.51	1.39	1.32

Table 4: Range and Estimated Mean Deflections by Districts

District	Observed Low	Estimated* Mean Value	Observed High
4	0.60	1.18	2.01
8	0.26	1.11	2.64
19	0.35	1.02	2.25
20	0.32	1.48	3.20
22	0.25	1.32	3.50
Overall	0.25	1.22	3.50

* Average of the mean values for 36 test points as predicted by the sine curve model fitted to the data.

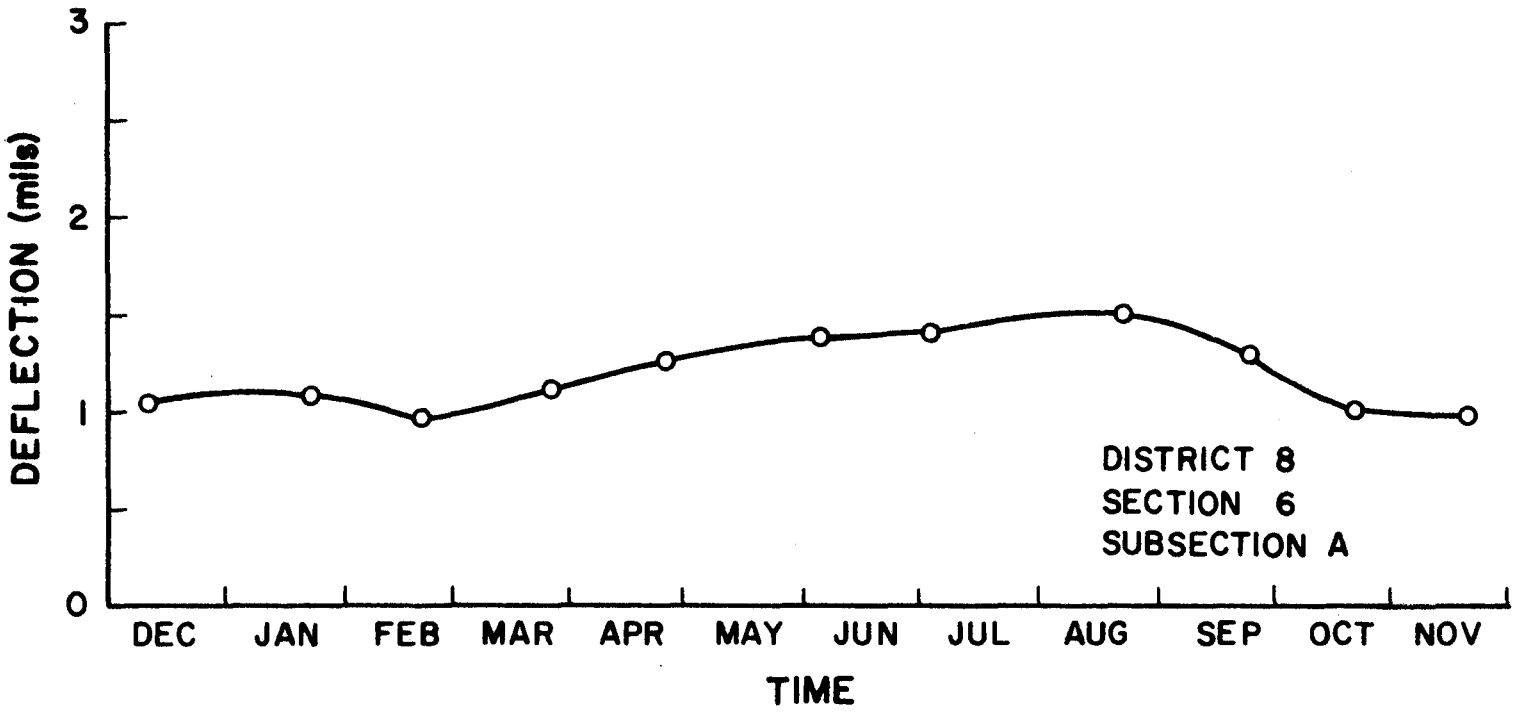

FIGURE 8 - Deflection curves like this one suggested a periodic variation, with maximum and minimum about six months apart.

Table 5: Results of Analyses of Variance Comparing Annual Subsection Maxima with Annual Subsection Minima

District	Number Subsections	Significantly* Different		Not Significantly Different	
		No.	Percent	No.	Percent
4	12	11	92	1	8
8	12	11	92	1	8
19	12	11	92	1	8
20	12	12	100	0	0
22	12	7	58	5	42
All	60	52	87	8	13

* at the 10% level

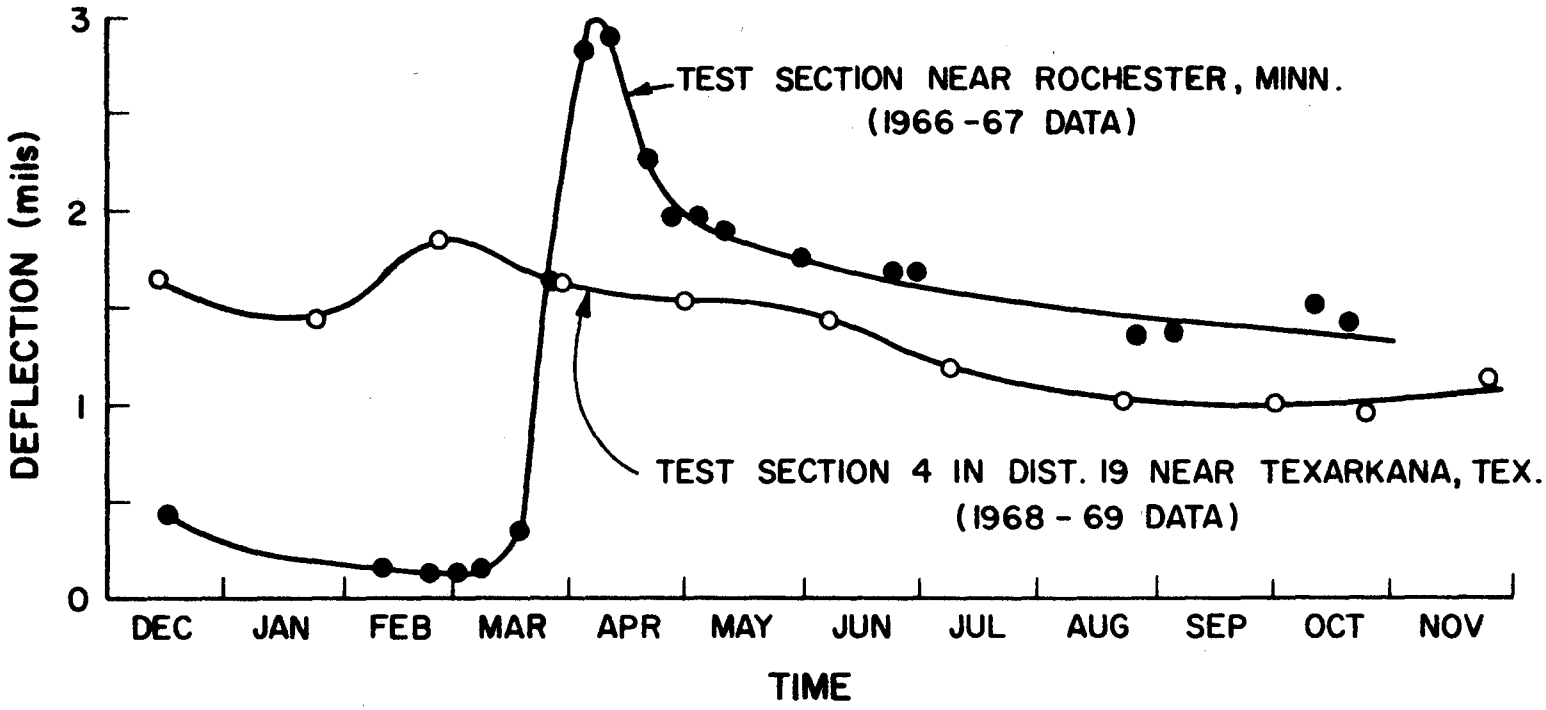

FIGURE 9 - Annual variations of deflections in Texas compared with those observed in Minnesota. Each point is the mean value for a 1000-ft. test section. The sharp rise in the Minnesota curve occurred during the spring thaw.

It is immediately evident from these curves that the variation of the Texas section deflections is not of the same type nor magnitude as that resulting from the freeze-thaw action indicated in the figure and commonly experienced in the northern United States.

4.2 Mathematical Model of Deflection As A Periodic Function of Time: Plots of deflection versus time, like those shown in Figures 8 and 9, indicated that the variations observed in Texas could be fitted with a sine wave having a period of one year. Such a curve, having the following equation, was fitted to the eleven observations made during the year on each of the 180 test points.

$$W_1(t) = A_1 + A_2 \sin \left[\frac{2\pi(t-A_3)}{365}\right] \qquad (1)$$

where $W_1(t)$ = the expected deflection in mils, at time t,

t = the time of year in days (t = 0 at midnight on December 31; $0 \leq t \leq 365$),

A_1 = the estimated mean annual deflection

A_2 = the amplitude of the sine curve = the difference between the estimated maximum (or minimum), and the mean annual deflection, and

A_3 = the time of year (days), during the period of increasing deflection, when $W_1(t) = A_1$.

The parameters A_1, A_2 and A_3 are illustrated graphically in Figure 10 which shows the observed deflection data and the fitted curve for test point 2 of section 6 in District 8. The expected time of occurrence of maximum deflection is represented by the symbol, T, where $T = A_3 + 91.25$ days. A non-linear regression technique developed by W. M. Moore and L. J. Milberger (4) was used to evaluate the set of constants, A_1, A_2 and A_3, for each of the 180 test points.

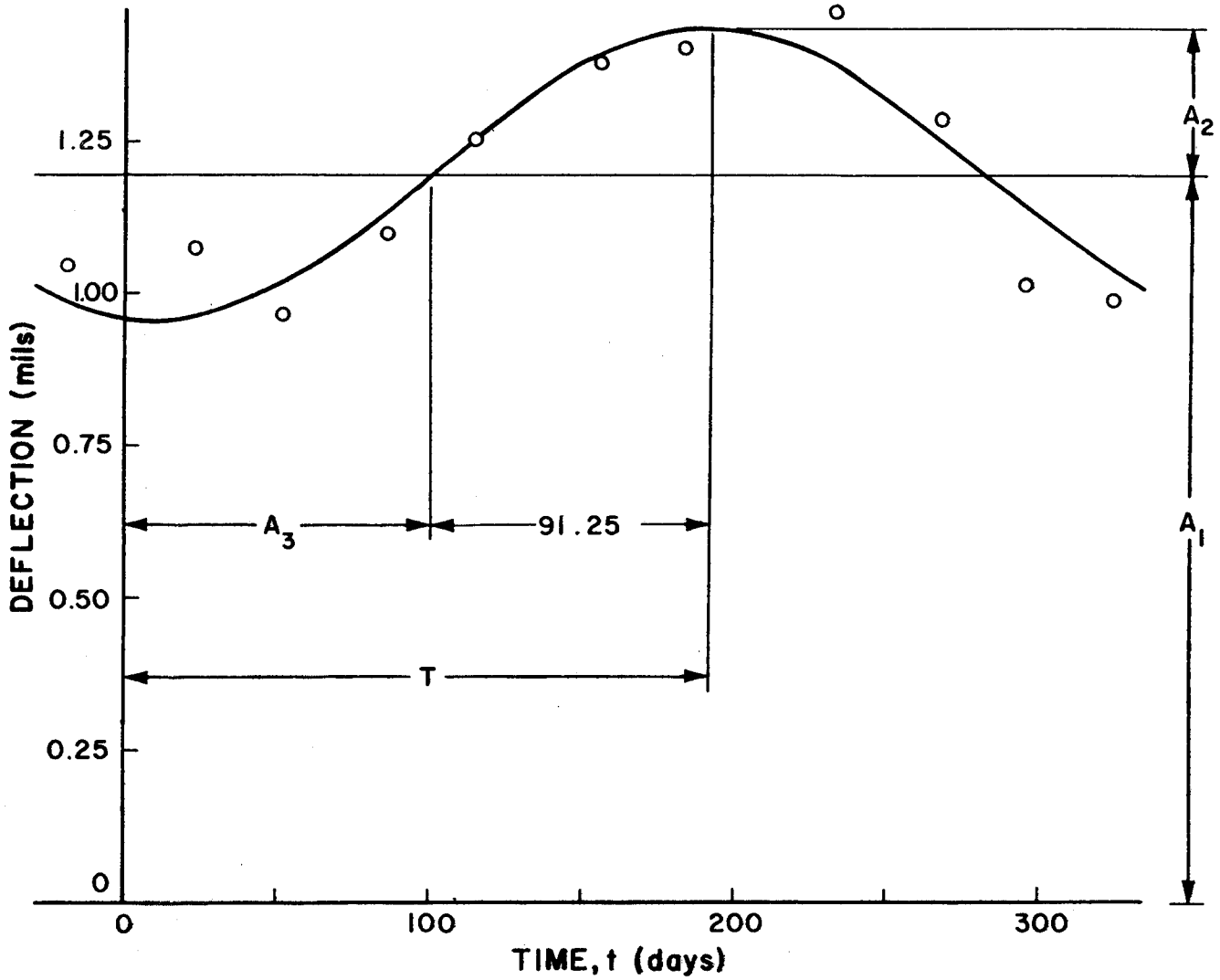

FIGURE 10 - Typical sine curve fitted to test point data. The parameters A_1, A_2 and T were analyzed with respect to test point location.

The fitted curve for any test point can be normalized by dividing the deflection equation by A_1, as exemplified in Figure 11. This procedure permits a direct comparison of estimated seasonal variations between sections having vastly different levels of deflection, and was made use of in some of the analyses to be described hereafter. The ranges of both actual and normalized variations of deflections encountered in this study are given in Table 6.

The distribution of the rather wide range of correlation coefficients resulting from fitting the 180 sine curves is shown in Figure 12. The correlation coefficients for well over one-half (61%) of the cases exceeded 0.80. It was less than 0.50 for only 8% of the cases.

An investigation of test points having low correlation coefficients revealed that the normalized amplitude (A_2/A_1) at these points was also low. Within equal intervals of A_2/A_1 (see Table 7), over the observed range, $0.011 \leq A_2/A_1 \leq 0.325$, the number of test points having correlation coefficients less than 0.80 was compared to the number having correlation coefficients equal to or greater than 0.80. These numbers were used to estimate, for each A_2/A_1 interval, the probability that the correlation coefficient will be equal to or greater than 0.80. The distribution of the probabilities is shown graphically in Figure 13. The number in each bar in this figure is the total number of data sources (test points) available for estimating the probability for the corresponding A_2/A_1 interval.

From the data shown in Figure 13, it may be concluded that if the normalized seasonal deflection variation at a test point is small, then the probability of obtaining a good sine wave fit is also small, while if the seasonal variation is large, the probability approaches unity.

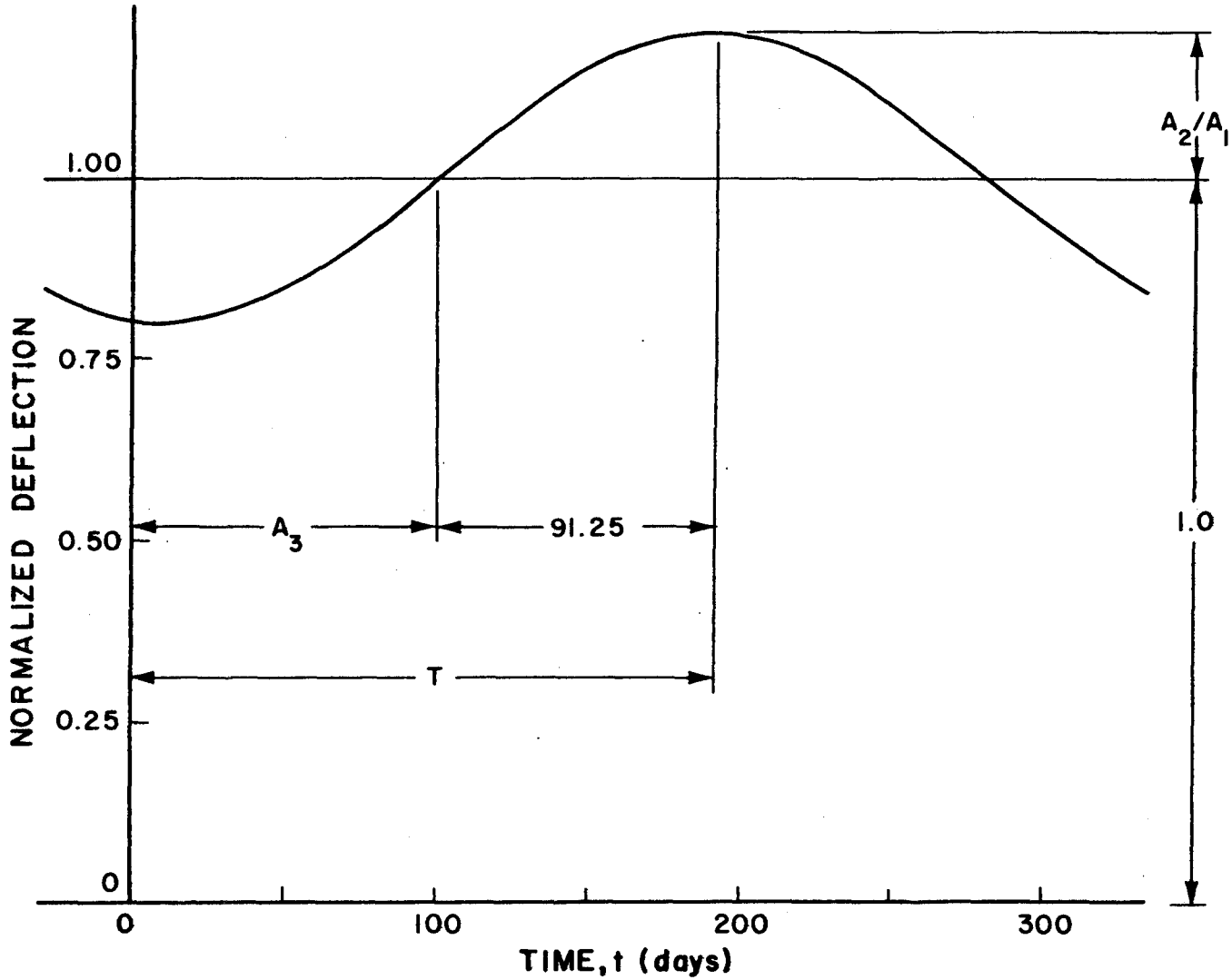

FIGURE 11 - Illustration of normalized amplitude (A_2/A_1) used for comparing data from test points located in different sections.

Table 6: Range of Estimated Annual Variations in Deflections

	Estimated Annual Variation*	
	Actual (mils) ($2A_2$)	Percent of Annual Mean ($\frac{2A_2}{A_1} \times 100$)
Minimum	0.014	2.2
Maximum	0.876	65.0

* The four figures in this table represent data from four different test points.

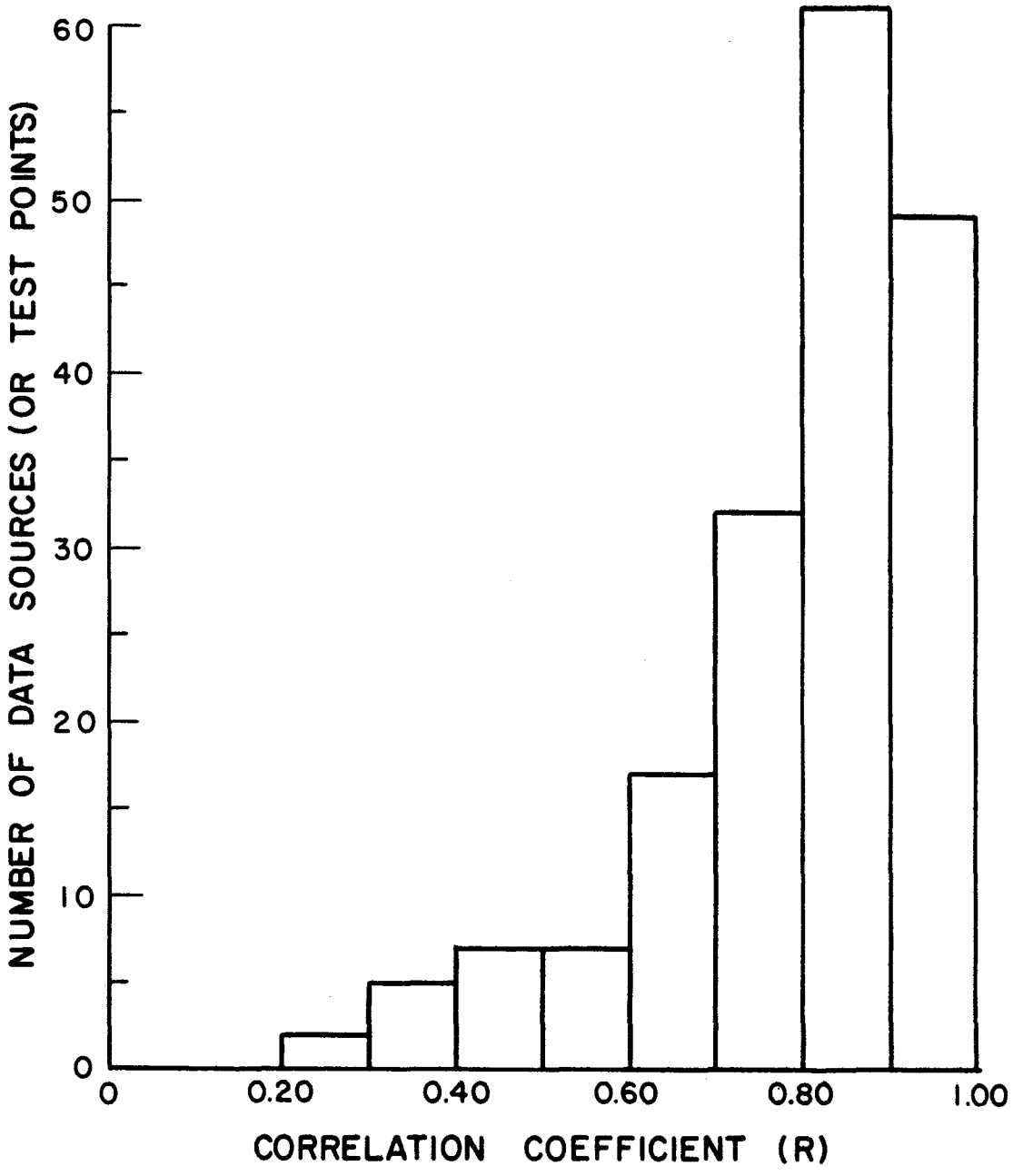

FIGURE 12 - Distribution of correlation coefficients obtained by fitting sine curves to data from the 180 test points.

Table 7: Probability of Achieving a "Good Fit" of a Sine Curve to the Deflection Data, as a Function of the Normalized Amplitude

A_2/A_1	No. Test Points			Prob.
	R* < 0.80	R ≥ 0.80	Total	R ≥ 0.80
0.000 - 0.024	6	0	6	0.00
0.025 - 0.049	26	1	27	0.04
0.050 - 0.074	21	19	40	0.48
0.075 - 0.099	13	34	47	0.72
0.100 - 0.124	2	23	25	0.92
0.125 - 0.149	1	8	9	0.89
0.150 - 0.174	1	3	4	0.75
0.175 - 0.199	0	7	7	1.00
0.200 - 0.224	0	6	6	1.00
0.225 - 0.249	0	3	3	1.00
0.250 - 0.274	0	4	4	1.00
0.275 - 0.299	0	1	1	1.00
0.300 - 0.325	0	1	1	1.00
Total	70	110	180	
Percent	39	61	100	

* Correlation coefficient

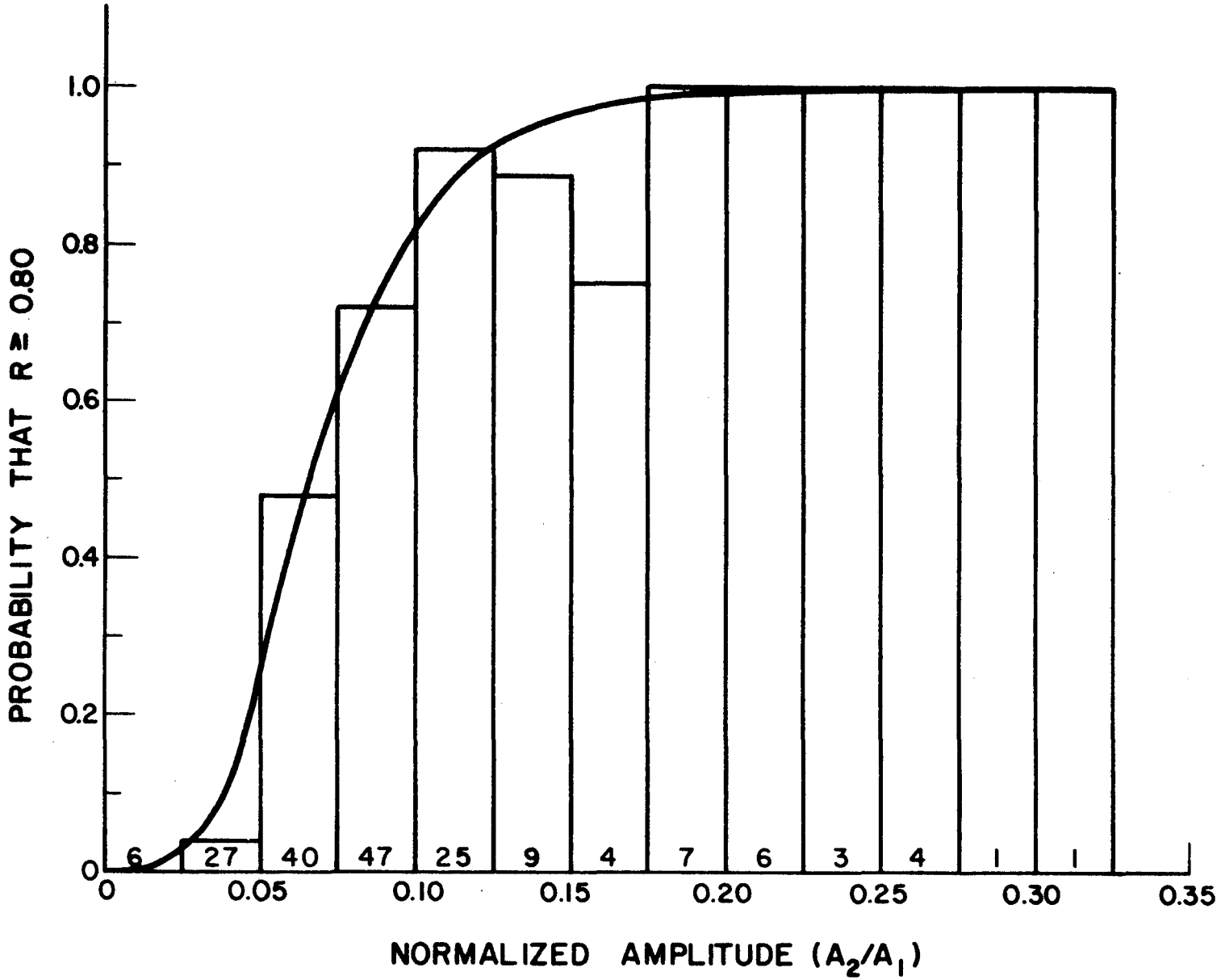

FIGURE 13 - Probability of achieving a "good fit" of a sine curve to the deflection data, as a function of the normalized amplitude.

This phenomenon may be explained by introducing the concept of random (i.e. unexplained) measurement errors that are proportional to the measured deflection. Such errors could overshadow real seasonal variations occurring at a point, if the latter are small compared to the mean annual deflection observed at that point.

4.3 Variation of Annual Mean Deflection, and Seasonal Change, with Test Point Location: Once the parameters A_1 (the mean annual deflection), A_2 (the amplitude, or one-half the annual change in deflection) and T (the time of maximum deflection) had been estimated for each of the 180 test points included in the experiment, it became possible to study the variation of these parameters with test point location. Variations of the mean annual deflection (A_1) and the annual deflection change ($2A_2$) are discussed in this section; the time (T) of occurrence of the maximum deflection is treated later (in Section 4.4). In establishing significant differences in A_1 or A_2 associated with differences in location, the analysis of variance was used, with significance determined at the 10% level.

4.3.1 Comparisons Between the Two Ends of A Section: Analyses of A_1 and A_2, comparing variability between the two subsections of a section with variability within the subsections, are discussed below.

Analyses of variance showed, for 21 of the 30 highway test sections, that the estimated annual average deflection, A_1, for the first 20-foot subsection was significantly different from that estimated for the second 20-foot subsection located only 1000 feet away. Also significantly different, for 19 of the same 30 sections, were the amplitudes, A_2, estimated for the two subsections.

From the results of these two analyses (Table 8) it may be said with respect to deflection measurements made at two points separated by a distance of only 1000 feet, on an apparently uniform pavement structure and foundation, that approximately two times out of three

(1) the mean annual deflection will differ significantly and

(2) the annual change in deflection will differ significantly.

These statements are based on the assumption that variations in a parameter (A_1 or A_2) determined at points separated by not more than twenty feet are random errors.

Another study of the differences between the two ends of a section, as compared to the seasonal variation observed at either end, led to the following conclusion: at a given instant, the difference between the deflections observed at the two ends of a 1000-foot section exceeded the total annual variation at either end of the section in 301 out of a total of 660 cases available for study. In other words, in 45 trials out of 100, a greater variation in deflection will be encountered by moving 1000 feet along a highway of apparently uniform strength than will be observed over a year's time at one point on the highway.

4.3.2 Comparisons Between the Six Sections within a District: Analyses of the normalized amplitude, A_2/A_1, were made comparing variations between the six sections in a district with variations within the sections. In each of the five districts, the normalized amplitudes of the six sections were found to be significantly different. These results imply that within a district, the annual percentage change in deflection may be expected to vary significantly from one highway to the next.

4.3.3 Comparisons Between Districts: Variations in A_2/A_1 between districts relative to the variations within the districts were compared

Table 8: Results of Analyses of Variance Comparing the Two Ends (Subsections) of a Section

District	A_1 (annual mean defl.)		A_2 (amplitude)	
	No. Sections Significantly Diff. at Ends	No. Sections Not Significantly Diff. at Ends	No. Sections Significantly Diff. at Ends	No. Sections Not Significant Diff. at Ends
4	3	3	4	2
8	3	3	5	1
19	6	0	3	3
20	4	2	5	1
22	5	1	2	4
Total	21	9	19	11

for all possible combinations of two districts. It was felt that differences between districts, if found to be significant, could be related to differences in temperature and/or rainfall. An analysis of variance was made comparing the normalized amplitudes estimated for the two districts of each combination. The results are presented in Table 9.

In addition, the average normalized amplitude for each district is shown on a Texas map in Figure 14, together with indications of significant differences between districts comprising the temperature-precipitation factorial experiment. It may be seen that the mean normalized amplitude of either of the two eastern districts is larger than that of any western district. However, the analyses of variance for the four-district factorial revealed that the normalized amplitudes in the eastern districts are significantly larger than those in the western districts in only three out of four cases. These results indicate that the annual percentage change in the deflections of a representative sample of highways in wet areas of the state will usually, but not always, be larger than in dry areas. Consistent trends between northern and southern districts could not be established.

4.4 Variation of Time of Maximum Deflection with Test Point Location: Analyses of variance similar to those described in Section 4.3 were made of the parameter, T (time of occurrence of maximum deflection) but, because of the cyclical nature of this variable, the results were not always clear-cut. It became obvious, after further study of the data, that the analysis of variance - which involved a manipulation of the deviations of a variable about its numerical mean - could not be

Table 9: Results of Analyses of Variance of A_2/A_1 (Normalized Amplitude) Comparing Districts by Pairs

Combination No.	Districts Compared	Significantly Different?
1	4, 8	No
2	4, 19	No
3	4, 20	Yes
4	4, 22	Yes
5	8, 19	No
6	8, 20	Yes
7	8, 22	Yes
8	19, 20	No
9	19, 22	Yes
10	20, 22	Yes

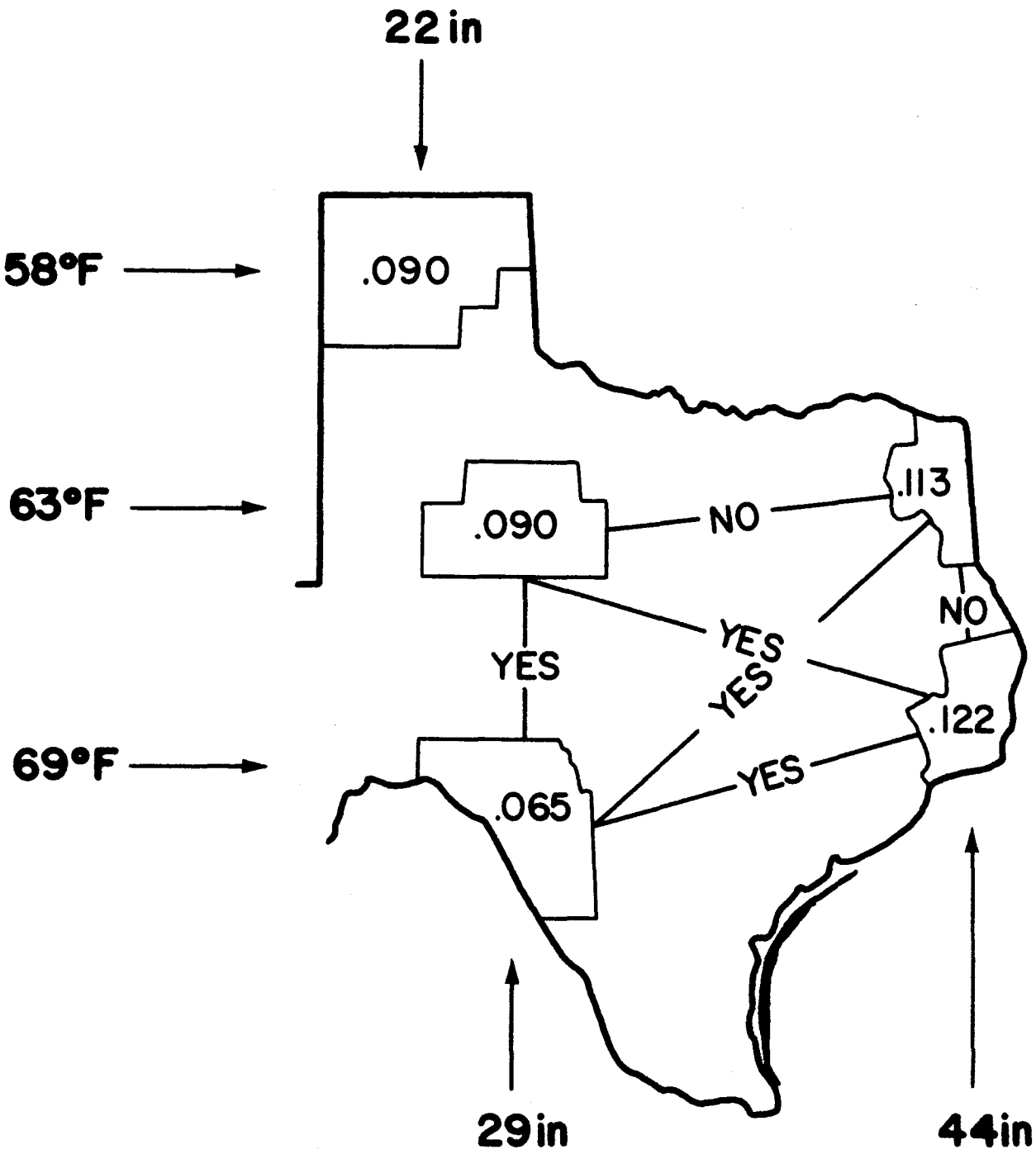

FIGURE 14 - Comparisons of mean normalized amplitudes between districts. A significant difference between two districts is indicated by YES printed on the line connecting the two.

easily applied to a variable whose value in some circumstances should be regarded as T, while in other circumstances it must be taken as T + 365, or perhaps as T - 365.

For example, in the upper portion of Figure 15 the 36 values of T observed in District 22 are plotted on the circumference of a circle divided into 365 equal parts. The first question to arise is - what is the mean or central value of T for District 22? This question was answered by resorting to a mechanical analogue: let the upper circle of Figure 15 represent a perfectly balanced wheel mounted on a frictionless, horizontal axle. To the rim of the wheel attach 36 equal weights at the points indicated by the plotted values of T. Now let the wheel come to rest under the influence of gravity, as shown in the lower part of Figure 15. Then the lowest point of the rim can be regarded as the "central value," $\tilde{T}$, for District 22.

Furthermore, the three-month interval with $\tilde{T}$ as its central value is the quarter with the greatest probability of having the highest occurrence of maximum deflections in District 22. The probability that a single observation taken at any point on a highway in this period will exceed the annual average deflection at that point, can be estimated by dividing the number of plotted points falling within the favored quarter by the total number observed in the district, 36. By the same procedure - counting and dividing - one can estimate the probability that a single observation taken in any other quarter will exceed the annual mean deflection.

To secure a measure of the density of the T-data in the vicinity of the central value, $\tilde{T}$, the analogy to mechanics was extended one step further: after the wheel came to rest, the torque required to rotate

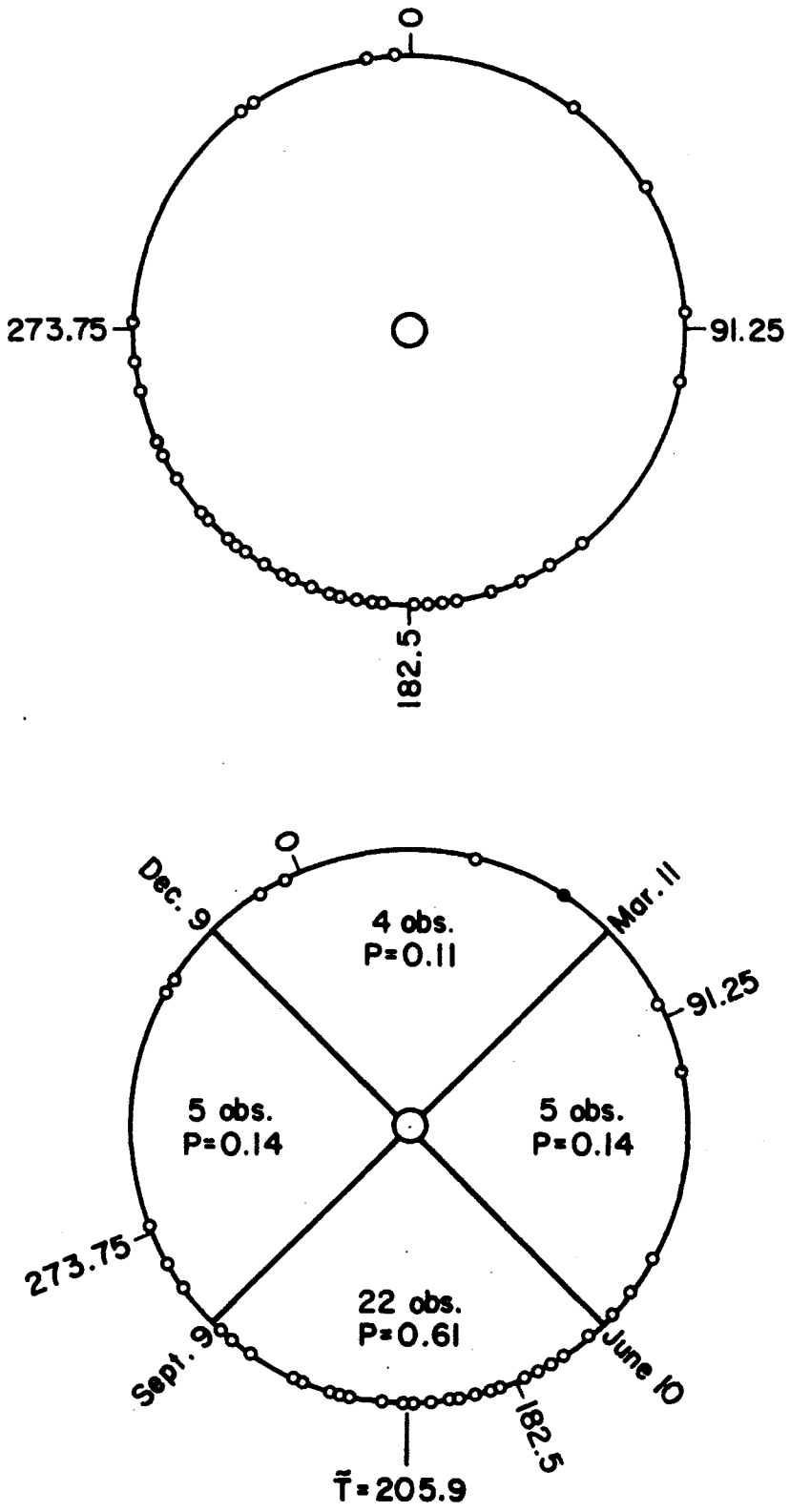

FIGURE 15 - Mechanical analogue used to find "central value," $\bar{T}$, of T-data. Upper: wheel with T-data represented by unit weights affixed to rim. Lower: wheel at rest under influence of gravity, with $\bar{T}$ at lowest point.

it through a small angle was divided by the torque that would have been required to move it through the same small angle had all the weights scattered about the rim been concentrated at the point, $T = \tilde{T}$. This quotient was termed the "grade," g, assigned to the data, its highest possible value being 1.0. The District 22 data used in this example had a grade of 0.51, the lowest of the five districts. In general, the grade of a set of T-data can be interpreted as a measure of the reliability of the central value, $\tilde{T}$.

The mathematical process used in finding the central value and the grade for the T-data of each district is easily derived, and is given in Appendix C. The results of the computations are given in Table 10, and are displayed graphically in Figure 16.

In Table 10, Quadrant 1 for each district is the three-month (or, more exactly, 91.25-day) period with its mid-date corresponding to the central value, $\tilde{T}$, for the district. Quadrant 2 is the next later quarter, etc. The district data are arranged in descending order of the grade, g, or reliability of the $\tilde{T}$-Data.

Also shown for each quadrant in Table 10 is the estimated probability that a deflection measured at a point within the district, and within the indicated limiting dates of the quadrant, will exceed the mean annual deflection at that point. Each quadrant and its probability is also displayed in Figure 16 as a shaded circular segment with radius proportional to the probability and angular width proportional to a quarter-year.

From Figure 16 it is apparent that there is a significant difference between the western and the eastern districts in the time of occurrence

Table 10: Probability that a Deflection Observed at a Point within a Given Three-Month Period Will Exceed the Mean Annual Deflection at that Point

District	Central Value, $\tilde{T}$	Grade, g	Quadrant	Limiting Dates		Estimated No. of Maximum Deflections	Estimated Probability
				From	To		
4	214.5	0.84	1	June 18	Sept. 18	29	0.81
			2	Sept. 18	Dec. 18	6	0.16
			3	Dec. 18	Mar. 19	0	0.00
			4	Mar. 19	June 18	1	0.03
20	126.6	0.79	1	Mar. 23	June 22	27	0.75
			2	June 22	Sept. 21	7	0.19
			3	Sept. 21	Dec. 21	0	0.00
			4	Dec. 21	Mar. 23	2	0.06
8	218.4	0.70	1	June 22	Sept. 22	27	0.75
			2	Sept. 22	Dec. 22	5	0.14
			3	Dec. 22	Mar. 23	1	0.03
			4	Mar. 23	June 22	3	0.08
19	102.9	0.62	1	Feb. 27	May 29	22	0.61
			2	May 29	Aug. 28	7	0.19
			3	Aug. 28	Nov. 28	1	0.03
			4	Nov. 28	Feb. 27	6	0.17
22	205.9	0.51	1	June 10	Sept. 9	22	0.61
			2	Sept. 9	Dec. 9	5	0.14
			3	Dec. 9	Mar. 11	4	0.11
			4	Mar. 11	June 10	5	0.14

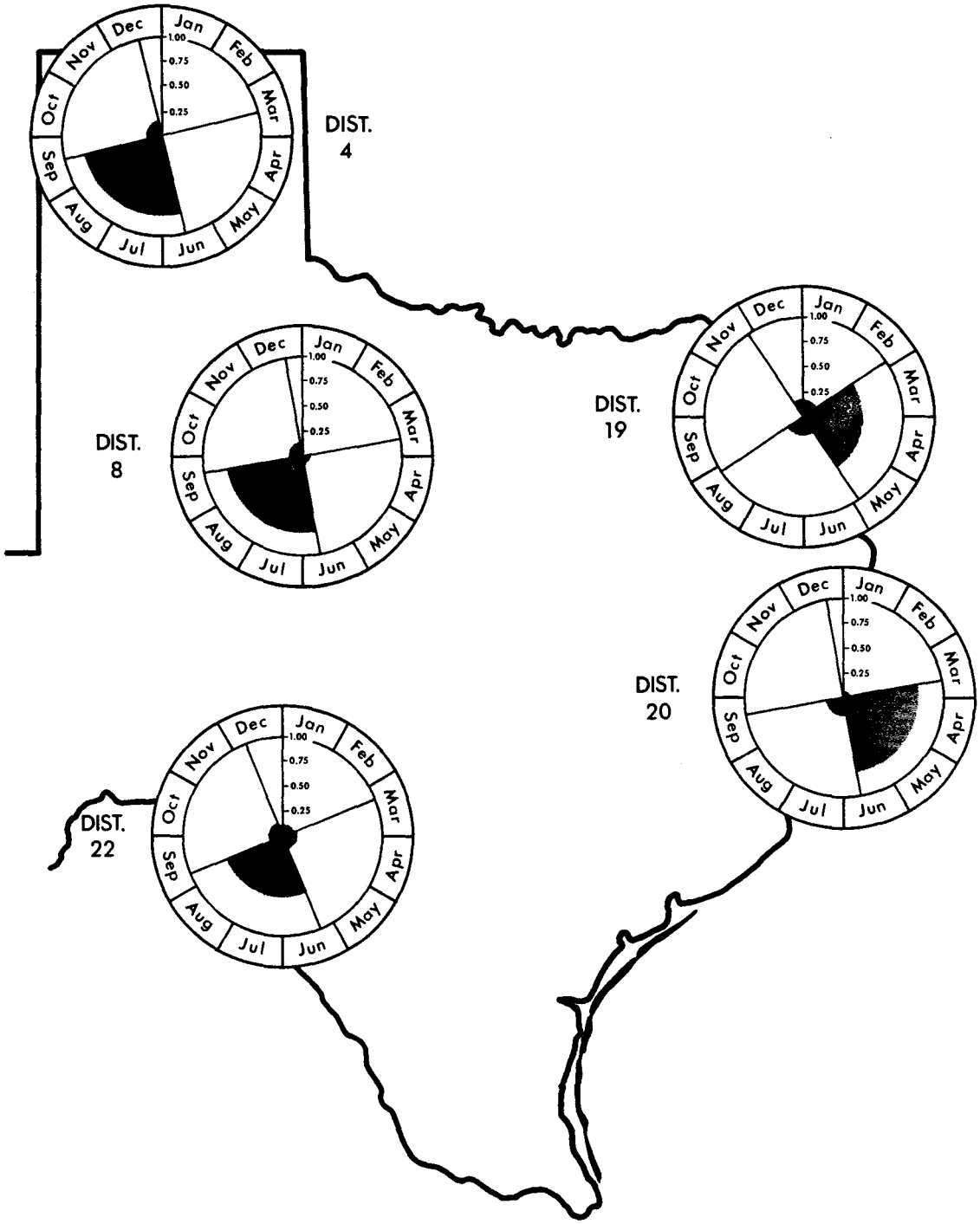

FIGURE 16 - Data from Table 10 plotted on annual clocks. Radii of shaded segments are proportional to probability of occurrence of above-average deflections.

of the maximum deflection, while there is no discernible trend between northern and southern districts having approximately the same rainfall. Thus, we must conclude that annual rainfall affects the timing of the annual maximum deflection at a point in Texas, while the mean annual temperature does not.

The findings illustrated in Figure 16 must be qualified somewhat insofar as they apply to the northernmost study area, District 4. It had been reported, prior to the beginning of the study, by personnel of that district that in some years, after a longer than usual period of freezing weather, severe pavement distress had been noted during the first two or three days following the advent of warmer weather. Thus in District 4, and perhaps in some other North Texas districts as well, the deflection-time curve in some years, for some pavements, may more nearly resemble the Rochester, Minnesota, curve shown in Figure 9 than the Texas pavement curve shown for comparative purposes in that figure. However, during this study - which extended from December, 1968, to November, 1969 - weather records show that the 1968-69 winter was milder than usual, a fact also reported during the progress of the study by District personnel. The rather mild winter in the Panhandle could account for the fact that no sudden and extreme increases in deflections were observed on the 36 test points in District 4.

That such sudden and brief increases might occur in District 4 was known to the researchers, who were in close touch by telephone with the district during the winter months, and were prepared to make special trips for the purpose of measuring these deflections. Apparently, however, they did not occur during the winter of 1968-69.

4.5 Summary of Findings: The findings reported in this chapter are summarized below.

1. The maximum deflection (mean of three test points) observed during the year on 52 of the 60 20-foot subsections was significantly greater than the minimum deflection.
2. A sine curve, with a period of one year, was found to be a suitable mathematical model of the variation with time of the deflection measured at a test point. In this sense, the deflections measured in this study contrasted sharply with those measured recently in the northern United States, where they usually increased from the annual minimum to the annual maximum within a period of about one month during the spring thaw.
3. With respect to deflections occurring at the two ends of a 1000-foot, apparently uniform test section, it may be said that the odds are about two to one that
   (1) the annual means of the deflections at the two ends will differ significantly, and
   (2) the annual changes in deflection at the two ends will differ significantly.
4. The odds are nearly even (45 to 55) that a greater variation in deflection will be found in the few minutes required to make a measurement at each of two points separated by 1000 feet of apparently uniform pavement and subgrade, than by making frequent measurements at one of the points over a period of one year. This finding logically leads to the inference that in a mile or more of pavement of the same design, the odds are much higher than even, that the variation in deflections

measured on the same day at intervals of say, 1000 feet, will exceed the annual variation at any one of the measuring points. If this inference is accepted, then it must be concluded that seasonal changes in the deflection of flexible pavements in Texas are usually less important than the random changes in the pavement-subgrade system that occur in distances that - from the designer's viewpoint - are relatively short (say one mile).

5. Within a district, the annual percentage change in deflection may be expected to differ significantly from one highway to the next.
6. The annual percentage change in deflection was usually greater in the eastern (wet) part of Texas, than in the western (dry) area.
7. The annual percentage change in deflection was significantly less in the southwestern district (District 22) than in the other four districts.
8. Deflections measured in the spring at a point in either of the two eastern districts tended to exceed the annual mean at that point; in the three western districts deflections tended to be highest in the summer. There was no discernible trend between northern and southern districts having approximately the same annual rainfall. It was concluded that annual rainfall is related to the timing of the annual maximum deflection at a point in Texas, while the mean annual temperature is not. (This finding however, is not intended to rule out the possibility that in some years, on some pavements, sudden, brief and extreme

increases in deflections will occur in the northern portions of the state, especially in the Panhandle, during the thaw following a protracted period of freezing weather.)

5. Significance of Findings to the Design Engineer

In the foregoing it was concluded that seasonal variations in the deflections of Texas pavements do exist, and that they tend to vary sinusoidally with time, with a period of one year. The findings, however, are of little interest to the design engineer unless they can be related - at least approximately - to the performance of pavements. An empirical mathematical model is available for this purpose and is, in fact, in use at the present time (on a trial basis) by several Texas Highway Department Districts in the new flexible pavement design system referred to in the Introduction (1).

5.1 Pavement Performance Model: The model (Equation 3, page 27 of Reference 1) relates serviceability loss to the "surface curvature index," to local temperatures, to the equivalent number of 18-kip single axle loads that have passed over the pavement, and to the action of swelling clays.

If the effect of swelling clays is neglected, the model can be written in the following form:

$$P = 5 - [\sqrt{5 - P_1} + 53.6NS^2/\alpha]^2 \qquad (2)$$

where P = the serviceability index of a pavement after N million applications of an 18-kip axle load,

P_1 = the initial serviceability index of the pavement,

S = the surface curvature index of the pavement, measured by Dynaflect ($S = W_1 - W_2$),

W_1 = reading of geophone no. 1 (mils) of the Dynaflect,

W_2 = reading of geophone no. 2 (mils) of the Dynaflect, and

$\bar{\alpha}$ = a temperature statistic for the Texas Highway Department District within which the pavement is located.

5.2 Seasonal Variations in the Surface Curvature Index: From Equation 2 it is evident that seasonal variations in the surface curvature index, S, must be known or estimated, if the effect of seasonal variations in deflections is to be evaluated in terms of the serviceability index. Although the variable, S, was measured in this study, it was not analyzed directly because it was much smaller than the variable W_1 (being the difference in the deflection of two points only one foot apart) and for this reason was subject to random measurement errors that were greater - in proportion to its own size - than was the deflection W_1. Thus the latter (W_1) was selected for studying changes of deflection with time, as indicated in the preceeding chapter.

However, it was known from previous research (Figure 29 of Reference 3) that some correlation exists between S and W_1, so that the surface curvature index at a test point could be expected in most cases to vary sinusoidally with time in phase with the deflection W_1. Thus, the maximum and minimum values of S at a test point could be expected to occur at approximately the same times as the maximum and minimum values of W_1.

5.2.1 Method of Estimating the Amplitude of S: It remained, however, to estimate the amplitude of the seasonal variation in S at each of the 180 test points included in the study. This was accomplished by following the step-by-step procedure outlined below for each test point.

1. A linear regression analysis was performed relating the S-data to the W_1-data. Because both variables were known to be subject

to random measurement errors, the procedure used was the "multiple error regression technique" developed by Scrivner and Moore (5). The "quality" of the two variables were assumed to be the same.

2. With the regression constants determined, the regression model was differentiated to find the numerical value of dS/dW_1.

3. The amplitude, ΔS, of the variable S was then estimated from the equation

$$\Delta S = \frac{dS}{dW_1} \cdot \Delta W_1 \qquad (3)$$

where ΔW_1 was the amplitude of W_1 determined as described in Chapter 4 and referred to in that chapter as the regression coefficient A_2.

5.2.2 Phase Relationship Between S and W_1: As a test of the hypothesis that the value of S at a test point varied in phase with W_1, the linear correlation coefficient, R, was computed in conjunction with each of the 180 regressions involved in Step 1, above. In about one-half (51%) of the cases, R exceeded 0.80. An investigation of test points having low coefficients ($R < 0.80$) revealed that the normalized amplitude of W_1 at these points was also relatively low. Within equal intervals of the normalized amplitude, $\Delta W_1/\bar{W}_1$, over the observed range, $0.011 \leq \Delta W_1/\bar{W}_1 \leq 0.325$, the number of test points having correlation coefficients less than 0.80 was compared to the number having correlation coefficients equal to or greater than 0.80. These numbers - as indicated in Table 11 - were used to estimate, for each $\Delta W_1/\bar{W}_1$ interval, the probability that the correlation coefficient will be equal to or greater

Table 11: Probability that the Linear Correlation of Surface Curvature Index (S) and Deflection (W_1) is "Good" ($R \geq 0.80$), as a Function of the Normalized Amplitude of W_1

$\Delta W_1/\bar{W}_1$	No. Test Points			Prob.
	R* < 0.80	R ≥ 0.80	Total	R ≥ 0.80
0.000 - 0.024	6	0	6	0.00
0.025 - 0.049	20	7	27	0.26
0.050 - 0.074	25	15	40	0.38
0.075 - 0.099	25	22	47	0.47
0.100 - 0.124	10	15	25	0.60
0.125 - 0.149	1	8	9	0.89
0.150 - 0.174	1	3	4	0.75
0.175 - 0.199	0	7	7	1.00
0.200 - 0.224	0	6	6	1.00
0.225 - 0.249	0	3	3	1.00
0.250 - 0.274	0	4	4	1.00
0.275 - 0.299	0	1	1	1.00
0.300 - 0.325	0	1	1	1.00
Total	88	92	180	
Percent	49	51	100	

* Correlation coefficient

than 0.80. The distribution of this probability is shown graphically in Figure 17. The number in each bar in this figure is the total number of data sources (test points) available for estimating the probability for the corresponding $\Delta W_1/\bar{W}_1$ interval.

From the data given in Table 11 and plotted in Figure 17, it may be concluded that if the normalized amplitude of the deflection W_1 at a test point is small, then the probability of there being good linear correlation ($R \geq 0.80$) between the surface curvature index, S, and the deflection, W_1, is also small, while if the normalized amplitude of W_1 is large, the probability of good correlation between S and W_1 approaches unity.

In more practical language, this simply means that where a strong seasonal variation in W_1 was observed (see Table 7 and Figure 13), there also existed a strong tendency for the surface curvature index, S, to vary throughout the year in phase with the deflection W_1 (see Table 11 and Figure 17). In the other cases it is the writers' supposition that the two quantities, S and W_1, were actually in phase, but the relationship was masked by experimental error.

5.2.3 The Amplitude of S: The results of following the step-wise procedure outlined in Section 5.2.1 above are summarized in Table 12. Each district mean given in this table is the average of data from 36 test points. The derivative dS/dW_1, and the estimated amplitude ΔS, were computed as previously described. The symbol $\bar{S}$, not previously defined, represents the mean annual value of S at a test point. The symbol σ represents the standard deviation of the quantity indicated.

From Table 12 it was concluded that (a) the change in surface curvature index per unit change in deflection (dS/dW_1) was greater, on

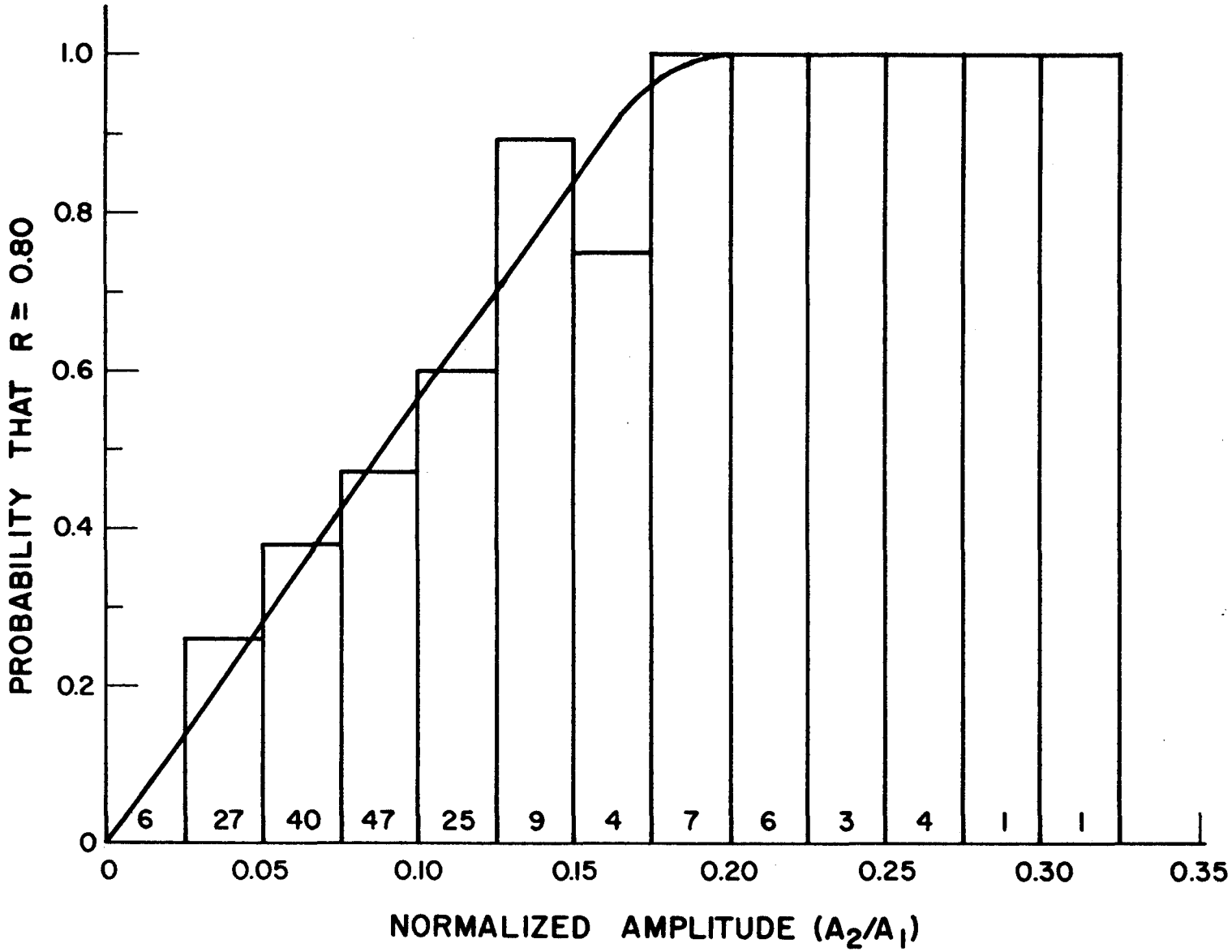

FIGURE 17 - Probability of good linear correlation between S and W.. as a function of the normalized

Table 12: Means and Standard Deviations, by Districts and Regions, of dS/dW_1, ΔS and $\overline{S}$

		dS/dW_1		ΔS*		$\overline{S}$	
Region	District	Mean	σ	Mean	σ	Mean	σ
West	4	0.75	0.21	0.07	0.04	0.42	0.13
	8	0.72	0.37	0.08	0.06	0.35	0.23
	22	0.78	0.23	0.06	0.06	0.48	0.36
	Regional Mean	0.75	0.27	0.07	0.05	0.42	0.24
East	19	0.54	0.16	0.06	0.05	0.28	0.11
	20	0.46	0.16	0.07	0.04	0.41	0.19
	Regional Mean	0.50	0.16	0.07	0.05	0.35	0.15
Both	All			0.07	0.05	0.39	0.23

* Computed from $\Delta S = \frac{dS}{dW_1} \cdot \Delta W_1$

the average, in the west than in the east, and (b) the amplitude, ΔS, of the seasonal variation in surface curvature index was, on the average, about the same in all the districts included in this study. The latter conclusion contrasts sharply with the finding reported in Chapter 4 that the normalized amplitude of the deflection, W_1, was generally greater in the eastern part of the state than in the west (see Figure 14).

5.2.4 Range of Variation of S: Table 13 was prepared from the means and standard deviations given in Table 12, and shows how the amplitude, ΔS, and the annual mean, $\bar{S}$, of the surface curvature index can be expected to vary within the areas included in this study. For example, it is estimated, based on Table 13, that, on the average, two out of any three test points selected at random on highways in District 4 will have amplitudes, ΔS, between 0.03 and 0.11 mils ($\Delta S = 0.07 \pm 0.04$ according to Table 12), and seasonal means, $\bar{S}$, between 0.29 and 0.55 mils ($\bar{S} = 0.42 \pm 0.13$ according to Table 12). Furthermore, two out of any three test points selected at random in the total area studied (five districts) will, on the average, have amplitudes between 0.02 and 0.12, and annual means between 0.16 and 0.62, as indicated in the last line of Table 13.

Study of the 180 pairs of values of ΔS and $\bar{S}$ revealed no consistent relationship between these two variables, other than the condition that $\bar{S} - \Delta S \geq 0$ (since negative values of S are not physically tenable). Therefore, in studying the possible effects on predicted values of the serviceability index of these seasonal variations, we must investigate a range of combinations of $\bar{S}$ and ΔS, where each quantity is varied independently, the only restriction being that $\Delta S \leq \bar{S}$. Then, for any

Table 13: Low and High Values of the Amplitude and the Annual Mean of Surface Curvature Index

Region	District	Amplitude, ΔS		Annual Mean, $\overline{S}$	
		$-\sigma$	$+\sigma$	$-\sigma$	$+\sigma$
West	4	0.03	0.11	0.29	0.55
	8	0.02	0.14	0.12	0.58
	22	0.00	0.12	0.12	0.84
East	19	0.01	0.11	0.17	0.39
	20	0.03	0.11	0.22	0.60
Both	All	0.02	0.12	0.16	0.62

selected combination, the corresponding maximum and minimum values of the surface curvature index can be calculated from the equations

$$\begin{aligned} Smax &= \bar{S} + \Delta S \\ Smin &= \bar{S} - \Delta S \end{aligned} \tag{3}$$

If values outside one standard deviation from the mean are excluded, a clue to the range over which $\bar{S}$ and ΔS may be expected to vary over the state is given in the last line of Table 13.

5.3 Variation of Other Variables in Equation 2: Besides the surface curvature index, three other variables, P_1, $\bar{\alpha}$ and N, must be quantified before Equation 2 can be used for estimating the effect on predicted values of the serviceability index of seasonal variations in deflections. For pavements surfaced with asphaltic concrete, the value of P can be expected to range from about 3.6 to about 4.8, according to Table 7 of Reference 6. Values of $\bar{\alpha}$ in Texas (a nine-year average) vary from 9° in District 4 to 38° in District 21, as indicated in Table 14. Values of N (the equivalent number of 18-kip axle loads) can vary widely, depending upon the highway and the length of time under consideration.

5.4 Sensitivity of Pavement Performance Model to Variations in S: For present purposes, P_1 was fixed at 4.2 and N was fixed at 0.10 (or 100,000 equivalent 18-kip axle loads) for all computations. Four values of $\bar{\alpha}$, 9°, 19°, 29° and 39°, were used, covering the range of this variable in Texas. Values of ΔS considered were based on the data presented on Table 13, and ranged from 0.01 to 0.16, while the values of $\bar{S}$ that were used varied from 0.10 to 1.00.

The results of the computations are given in Table 15. In this table is shown the difference, ΔP, in the predicted serviceability index

Table 14: Values of the Temperature Statistic, $\bar{\alpha}$, by Districts*

Dist.	$\bar{\alpha}$	Dist.	$\bar{\alpha}$	Dist.	$\bar{\alpha}$	Dist.	$\bar{\alpha}$	Dist.	$\bar{\alpha}$
1	21	6	23	11	28	16	36	21	38
2	22	7	26	12	33	17	30	22	31
3	22	8	26	13	33	18	26	23	25
4	9	9	28	14	31	19	25	24	24
5	16	10	24	15	31	20	32	25	19

* Reproduced from Table 1, Reference 1 .

Table 15: Values of ΔP for Various Combinations of $\bar{\alpha}$, $\bar{S}$ and ΔS, with P_1 Fixed at 4.2 and N at 0.10

$\bar{\alpha} = 9$	$\bar{S}$			
ΔS	0.10	0.40	0.70	1.00
0.01	0.004	0.019	0.040	0.071
0.06	0.026	0.113	0.238	0.427
0.11	-	0.209	0.438	0.785
0.16	-	0.306	0.641	1.147

$\bar{\alpha} = 19$	$\bar{S}$			
ΔS	0.10	0.40	0.70	1.00
0.01	0.002	0.008	0.016	0.027
0.06	0.012	0.051	0.098	0.159
0.11	-	0.094	0.180	0.293
0.16	-	0.137	0.263	0.427

$\bar{\alpha} = 29$	$\bar{S}$			
ΔS	0.10	0.40	0.70	1.00
0.01	0.001	0.005	0.010	0.016
0.06	0.008	0.033	0.061	0.096
0.11	-	0.060	0.112	0.176
0.16	-	0.088	0.164	0.256

$\bar{\alpha} = 39$	$\bar{S}$			
ΔS	0.10	0.40	0.70	1.00
0.01	0.001	0.004	0.007	0.011
0.06	0.006	0.024	0.044	0.068
0.11	-	0.044	0.082	0.125
0.16	-	0.065	0.119	0.182

of an existing pavement that would result if one first used a minimum value (Smin) of the surface curvature index, measured on the pavement during a period of low deflections, and then later used a maximum value (Smax), measured during a period of high deflections.

Values of ΔP were computed from the following equation derived from Equation 2, with $P_1 = 4.2$ and $N = 0.10$:

$$\Delta P = [\sqrt{0.8} + 5.36\ S\bar{max}^2/\bar{\alpha}]^2 - [\sqrt{0.8} + 5.36\ S\bar{min}^2/\bar{\alpha}]^2 \qquad (4)$$

where Smax and Smin were computed from Equations 3 using the values given in the margins of Table 15. The values of $\bar{\alpha}$ used are given in the upper left corner of each of the four sections of the table.

The values of ΔP in Table 15 should be interpreted in the light of the measurement error associated with the serviceability index, P. This error is believed to be at least $\pm$ 0.10, and probably greater. Therefore, values of ΔP less than about 0.2 in Table 15 should be regarded as having no practical significance, since they probably could not be detected by actual measurement. Values greater than 0.2 in Table 15 have been underlined. By noting the frequency of the underlined figures in the four sections of the table it can be seen that when $\bar{\alpha}$ equals or exceeds 19°, a significant error in the predicted value of the serviceability index after 100,000 applications of an 18-kip axle load can be expected only for a pavement having a greater-than-average annual mean value of surface curvature index, and then only if the pavement also has a greater-than-average seasonal variation, ΔS, in the surface curvature index.

On the other hand, in areas where $\bar{\alpha}$ is less than 19°, larger differences in the predicted values of the serviceability index of existing pavements can be expected. Furthermore, had Table 15 been prepared using a value of N greater than 0.10, it can be shown that

the values of ΔP for all values of $\bar{\alpha}$ would have been greater and more of them would have exceeded the significant difference of 0.2. The conclusion that must be drawn from these considerations is that the safest course for the design engineer using the current version of the flexible pavement design system is to attempt to measure deflections when they are most likely to exceed their annual mean.

In view of the many uncertainties associated with seasonal deflection variations, an alternate, and, in the long run, perhaps a more practical procedure than that recommended in the preceding paragraph would be to introduce seasonal variations in deflections as a random (unexplained) variable in the flexible pavement design system computer program. This approach would entail the study of this variable in conjunction with several others of the many variables used in the program that exhibit random variations. Such a study is considered to be beyond the scope of this report; however, all the data gathered in this research are stored on IBM cards at Texas Transportation Institute, and are available, when required, for use in any subsequent effort to modify the flexible pavement design system to include a random variable to represent seasonal variations in deflections.

5.5 Summary of Findings: The findings reported in this chapter are summarized below.

1. At a test point where a pronounced seasonal variation in the deflection, W_1, was observed, there also existed a strong tendency for the surface curvature index, S, to vary in phase with the deflection. At points where seasonal variations in deflection were relatively small, the in-phase relationship was apparently masked by experimental error.

2. The change in surface curvature index per unit change in deflection (dS/dW_1) was greater, on the average, at test points in the west than in the east, but the amplitude, ΔS, of the seasonal variation in surface curvature index was, on the average, about the same in all areas.
3. According to predictions calculated from the pavement performance model used in the flexible pavement design system now on trial in several districts, it appears that the safest course for the design engineer using that system as it now exists is to attempt to measure deflections during the three-month period when deflections are most likely to exceed their annual mean.
4. An alternate and, in the long run, perhaps a more practical procedure than that recommended in the preceding paragraph, would be to modify the current version of the flexible pavement design system computer program to receive a random (unexplained) variable to represent seasonal variations in deflections. The work of modifying the program is considered to be beyond the scope of this research. Some of the necessary basic data have been collected in this study, are stored on IBM cards at Texas Transportation Institute, and are readily available when required.

6. Assumed Relationship of Annual Rainfall to Time of Highest Deflections

As a possible aid to the designer in selecting a time when deflections are most likely to exceed their annual mean, the mid-date of the three-month period having the highest deflections for each district, and the annual rainfall for that district, are given in Table 16 and plotted in Figure 18. The inference of Figure 18 is that in areas of light rainfall in Texas (less than 30 inches per year) high deflections can be expected to occur in the warmest season of the year, while in areas of heavier rainfall, high deflections will occur somewhat earlier - as much as three months earlier near the Louisiana border where annual precipitation is greatest.

The authors have attempted to find a clear-cut physical explanation of the apparent relation of rainfall to the annual deflection cycle, in terms of variations with time, within each district, of temperature, rainfall, humidity, river discharge, depth of water table, etc., but with little success. It was, therefore, with some misgivings, that Figure 18 was included in this report. However, that figure is the only general guide to the annual deflection cycle in Texas that could be devised based on the data collected in this study.

Table 16: Annual Rainfall Data and Mid-date of Quarter Having Highest Deflections

strict	Weather Stations	Annual Rainfall, In.	Mid-date
4	Amarillo, Borger, Canyon, Claude, Dumas, Panhandle	22.5	August 3
8	Colorado City, Hamlin, Roby, Roscoe, Rotan, Winters	28.1	August 7
22	Amistad Dam, Brackettville, Carta Valley, Del Rio, Eagle Pass, La Pryor, Uvalde	29.1	July 25
19	Atlanta, DeKalb, Texarkana, Texarkana Dam	43.5	April 13
20	Beaumont, Port Arthur	45.1	May 7

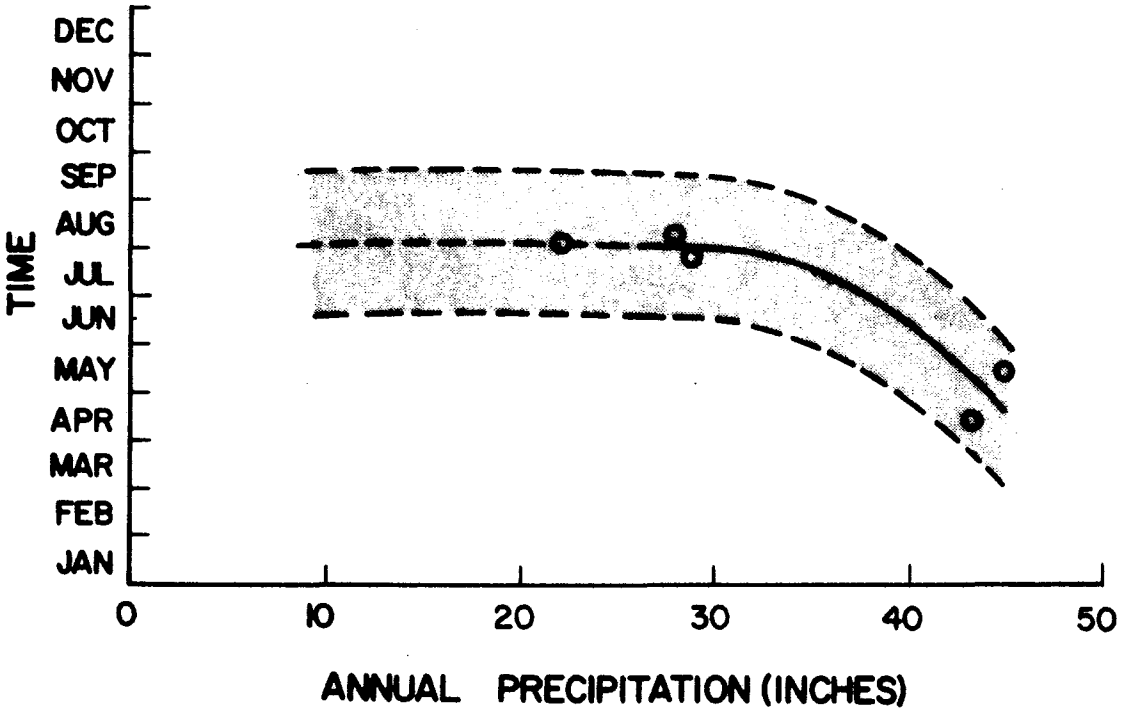

FIGURE 18 - Central dates of quarter having highest deflections, plotted against annual rainfall. Shaded band is assumed to represent best period for measuring deflections for design purposes.

List of References

1. Scrivner, F. H.; Moore, W. M.; McFarland, W. F.; and Carey, G. R. "A Systems Approach to the Flexible Pavement Design Problem," Research Report 32-11, Texas Transportation Institute, 1968.

2. Scrivner, F. H.; Swift, Gilbert; and Moore, W. M. "A New Research Tool for Measuring Pavement Deflection," Highway Research Record No. 129, Highway Research Board, Washington, D. C., pp. 1-11, 1966.

3. Scrivner, F. H.; Poehl, Rudell; Moore, W. M.; and Phillips, M. B. "Detecting Seasonal Changes in Load-Carrying Capabilities of Flexible Pavements," NCHRP Report 76, Highway Research Board, Washington, D. C., 1969.

4. Moore, W. M. and Milberger, L. J. "Evaluation of the TTI Gyratory Compactor," Research Report 99-3, Appendix D, Texas Transportation Institute, 1968.

5. Scrivner, F. H. and Moore, W. M. "Evaluation of the Stiffness of Individual Layers in a Specially Designed Pavement Facility from Surface Deflections," Research Report 32-8, Appendix B, Texas Transportation Institute, 1966.

6. Scrivner, F. H. and Michalak, Chester H. "Flexible Pavement Performance Related to Deflections, Axle Applications, Temperature and Foundation Movements," Research Report 32-13, Texas Transportation Institute, 1969.

7. "Operators Manual for the Dynaflect," Radiation, Engineering and Manufacturing Co. (REMCO), 7450 Winscott Rd., Fort Worth, Texas.

Appendix A
Test Procedures

This appendix contains the procedures for the measurements made on the individual test sections. It includes procedures for measuring Dynaflect deflections and temperatures. Six test points, numbered 1 to 6 in the direction of traffic flow, were permanently marked in the outer wheel path of each test section so that testing could be done at precisely the same points during successive visits (Figure 2). These test points are referenced in the procedures below.

Dynaflect Operating Procedure

The procedure used to obtain the Dynaflect deflections is divided into two parts, (a) the calibration procedure and (b) test section measurements. Calibration was normally done upon arriving at each test section. A more detailed operating procedure as well as the steps to be followed when malfunctions occur are contained in the manufacturer's operations manual (7).

(a) Calibration Procedure:

1. Connect the calibrator to control unit. Connect five sensors to their mating connectors and put sensors 1 through 4 in the calibrator.
2. Turn on power switch and allow control unit to warm up. Place frequency toggle switch in "CALIBRATE" position, sensor toggle switch in "DOWN" position, and deflection multiplier in "CAL" position. Adjust calibrator control frequency to 8 cps.

3. Place sensor selector switch to position 1 and adjust sensor 1 trim knob so that the deflection meter reads at the "CAL" position. Lock sensor 1 trim knob.
4. Place sensor selector switch to position 2. Adjust and lock sensor 2 trim knob. Similarly adjust sensors 3 and 4. Turn off sensor selector switch.
5. Replace one of sensors in the calibrator with sensor 5 and adjust sensor 5 using the same procedure as used for sensors 1 through 4.
6. Recheck frequency meter and readings for the sensors in calibrator. Place sensor toggle switch in "UP" position.
7. Disconnect and stow the calibrator.

(b) Test Section Measurements:

1. Place identification of section, date, etc., on Dynaflect data sheet.
2. Screw triangular bases on sensors and connect the sensors to the sensor carriage.
3. Place frequency toggle switch to "OPERATE" position and force toggle switch to "DOWN" position.
4. Pull onto pavement and center on outer wheel path.
5. Drive to first test point.
6. Place sensor switch in "DOWN" position and adjust frequency to 8 cps.
7. Place sensor selector switch in position 1 and adjust multiplier switch for maximum reading. Record deflection

meter reading and multiplier switch setting on data sheet. Repeat procedure for sensors 2 through 5. Turn off sensor selector switch.

8. Place sensor switch in "UP" position.
9. Repeat steps 5 through 8 for test points 2 through 6.
10. Drive off pavement and place force switch in "UP" position.
11. Turn off power switch, disconnect and stow sensors.

Temperature Measurement Procedure

The procedure described in this section is used to obtain subsurface temperatures. Thermocouples were made with copper and constantan wires. Connection to thermocouples for measurement was made to a stationary connector located on the highway shoulder. The thermocouples were read with a Leeds and Northrup potentiometer having direct temperature readout.

1. Upon arrival at the beginning of the test section, plug thermocouple lead from potentiometer into connector on highway shoulder.
2. Place the surface thermocouple lead on the pavement with the surface probe in contact with the pavement.
3. Record air temperature.
4. Zero and calibrate potentiometer.
5. Read and record temperature for all thermocouples.
6. Repeat steps 1 through 5 at the end of the section (after measuring deflection on test point 6).

Appendix B
Temperature and Precipitation Data

This appendix contains a discussion of air temperatures and precipitation rates during the test period obtained from climatological data files, and ground temperatures measured by thermocouples.

Average monthly air temperatures and total monthly precipitation rates for each district are given in Table 17. The temperature data were taken from a weather station centrally located with respect to the six sections in each district. The following weather stations were used.

District	Weather Station
4	Amarillo
8	Roscoe
19	Texarkana
20	Port Arthur
22	Brackettville

Since precipitation throughout the district was much more variable than temperature, the monthly precipitation rates from a number of weather stations in the general vicinity of the six test sections located in each district were averaged and these averages are the values shown in the table. The weather stations used in determining precipitation in each district have been previously listed in Table 16 of Chapter 6.

An examination of the 12-month means in the last column of Table 17 reveals a definite north-south trend in temperature and east-west trend in precipitation. The conditions of the temperature-precipitation

Table 17: Climatological Data for 12-Month Test Period

	Dist.	Dec. 1968	Jan. 1969	Feb. 1969	Mar. 1969	Apr. 1969	May 1969	June 1969	July 1969	Aug. 1969	Sep. 1969	Oct. 1969	Nov. 1969	12-mo. mean
Average Monthly Air Temperature (°F)	4	37	41	40	39	60	67	73	83	80	71	54	47	58
	8	46	49	48	47	65	70	79	86	83	73	61	53	63
	19	45	46	46	47	63	71	77	85	82	76	66	53	63
	20	54	55	55	55	69	75	81	85	83	78	72	60	69
	22	51	54	56	56	71	75	83	87	86	79	69	56	69

														12-mo. total
Total Monthly Precipitation (inches)	4	0.15	0.02	0.91	1.52	0.22	4.20	3.57	2.44	2.66	3.64	2.79	0.36	22.5
	8	0.41	0.21	1.15	1.70	2.30	5.95	2.14	0.24	2.47	7.00	3.03	1.47	28.1
	19	3.97	4.04	4.83	5.94	4.04	5.19	1.08	2.13	1.22	2.04	3.96	5.09	43.5
	20	3.39	1.16	5.63	3.43	6.32	5.97	1.63	9.51	2.93	1.23	2.08	1.82	45.1
	22	0.42	0.72	1.24	0.51	3.46	3.94	1.11	0.89	3.72	1.52	8.62	2.91	29.1

factorial experiment involving Districts 8, 19, 20 and 22 were satisfied.

A study of the ground temperatures, measured at both ends of each section during each visit, and only during daylight hours, indicate that the temperature at a given depth within each test section pavement was essentially uniform throughout the section length. However, a definite difference in temperature was observed at different depths within a section. In general, at a given time during the winter, the temperature increased with depth, while the opposite was observed in the summer. These trends were not necessarily observed at depths near the surface that were influenced by daily air temperature fluctuations. A comparison of temperatures measured at any given depth in a section at different times during the test period yields the expected results; the highest temperatures occur during the summer months and the lowest during the winter months.

Pavement temperatures below 32°F were measured during only one visit on January 23, 1969, and then only on two sections. While the air temperature was approximately 22°F, the surface temperature of sections 4 and 5 in District 4 was measured at 30°F. However, the temperature measured 4 inches below the surface was 36°F.

Temperatures on the pavement surface, and at 36 inches below the surface, respectively, of the six sections in each district were averaged for each visit to permit a comparison of temperature trends between districts. These district averages are shown in Table 18 and plotted against time in Figure 19. Each number in the table, or data point in the figure is the average of 12 readings, one at each

Table 18: Mean Thermocouple Temperature Data for 12-Month Test Period

		Dates Measured*										
	Dist.	Dec. 9-16, 1968	Jan. 21-27, 1969	Feb. 18-25, 1969	Mar. 24-31, 1969	Apr. 22-30, 1969	June 2-9, 1969	June 30-July 8, 1969	Aug. 18-25, 1969	Sept. 22-30, 1969	Oct. 20-27, 1969	Nov. 18-25, 1969
Temperature on top of Pavement Surface (°F)	4	48	40	39	66	87	103	116	104	82	49	60
	8	65	72	53	76	100	86	118	112	93	61	61
	19	56	46	66	78	89	100	114	89	90	70	70
	20	55	76	82	96	103	114	112	108	106	98	67
	22	66	74	71	77	95	95	110	118	99	93	63
Temperature 36-inches below Pavement Surface (°F)	4	52	50	48	53	66	78	86	92	81	68	60
	8	59	59	56	61	72	83	90	97	86	77	69
	19	60	57	57	64	74	85	97	96	89	80	67
	20	64	65	63	70	77	84	94	94	91	84	71
	22	66	65	65	67	78	87	93	99	91	83	74

* Measurements at each subsection were made within a 5-minute period at some time between 8 A. M. and 6 P. M.

FIGURE 19a - Surface and subgrade temperature versus time curves for the four districts comprising a temperature-precipitation factorial experiment. Each data point is the average of 12 observations, one at each subsection. The open circles are surface temperatures and the dark circles are subgrade temperatures 36-inches below the surface.

TEMPERATURE (°F)
20
40
60
80
100
120
DEC
JAN
FEB
MAR
APR
MAY
JUN
JUL
AUG
SEP
OCT
NOV
TIME
DISTRICT 22

TEMPERATURE (°F)
20
40
60
80
100
120
DEC
JAN
FEB
MAR
APR
MAY
JUN
JUL
AUG
SEP
OCT
NOV
TIME
DISTRICT 8

TEMPERATURE (°F)
20
40
60
80
100
120
DEC
JAN
FEB
MAR
APR
MAY
JUN
JUL
AUG
SEP
OCT
NOV
TIME
DISTRICT 20

TEMPERATURE (°F)
20
40
60
80
100
120
DEC
JAN
FEB
MAR
APR
MAY
JUN
JUL
AUG
SEP
OCT
NOV
TIME
DISTRICT 19

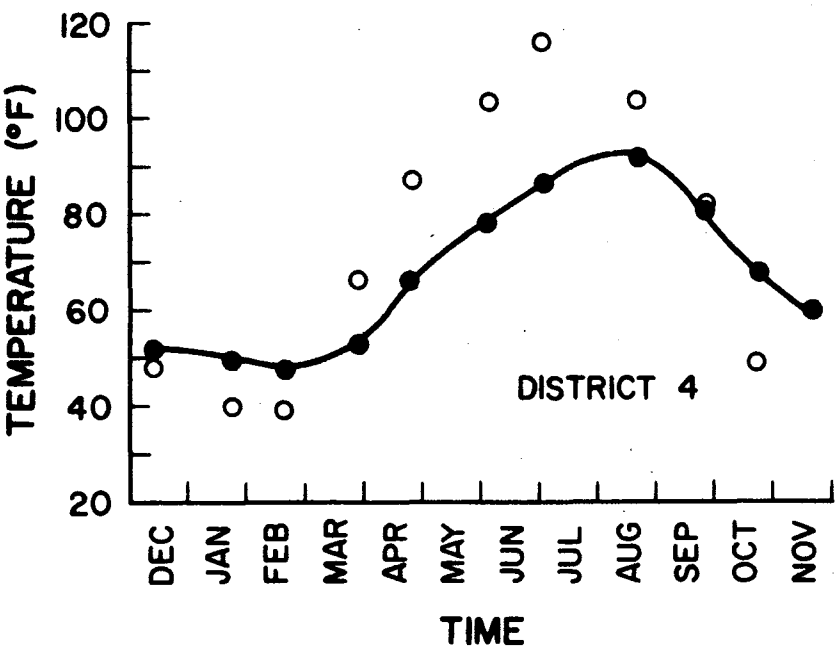

FIGURE 19b - Surface and subgrade temperature curves for District 4. Each data point is the average of 12 observations, one at each subsection. The open circles are surface temperatures and the dark circles are subgrade temperatures 36-inches below the surface.

subsection. The temperatures measured 36 inches below the surface (dark circles) exhibit a distinct seasonal trend. The seasonal trend shown by the surface temperatures, represented by open circles, is more erratic because of the influence of daily air temperature fluctuations.

The average monthly air temperatures from Table 17 (triangles) and the average temperatures at 36 inches below the pavement surface from Table 18 (circles) are plotted against time for each district in Figure 20. In all five districts, the shapes of the two temperature curves are very much alike. The average monthly air temperature was always less than the 36 inch deep pavement temperature.

The four districts represented in Figure 20a are those chosen for an evaluation of the effects of temperature and precipitation rate on deflection. Based on a study of the data used in these four district plots, it may be said of the average monthly air or 36-inch deep pavement temperature that (a) no consistent north-south or east-west trends of maximum temperature were observed, (b) the minimum temperatures in the two northern districts - 8 and 19 - were lower than the minimum temperatures in the two southern districts - 20 and 22 - and therefore, (c) the seasonal temperature change - range - was larger in the two northern districts than in the two southern districts. The average monthly air temperature ranges are shown on the district maps in Figure 21 and the observed 36-inch deep temperature ranges in Figure 22. These ranges for District 4 are also included.

From the data given in Figures 21 and 22 it may be concluded that the annual range of temperature variation measured 36 inches below the pavement surface at a given location in Texas is very nearly the same as the annual range of the average monthly air temperature at that location.

FIGURE 20a - Average monthly air and subgrade temperature versus time curves for the four districts comprising a temperature-precipitation factorial experiment. Each subgrade data point is the average of 12 observations, one at each subsection. The air temperatures are from climatological data files. The circles are subgrade temperatures 36 inches below the surface and the triangles are air temperatures.

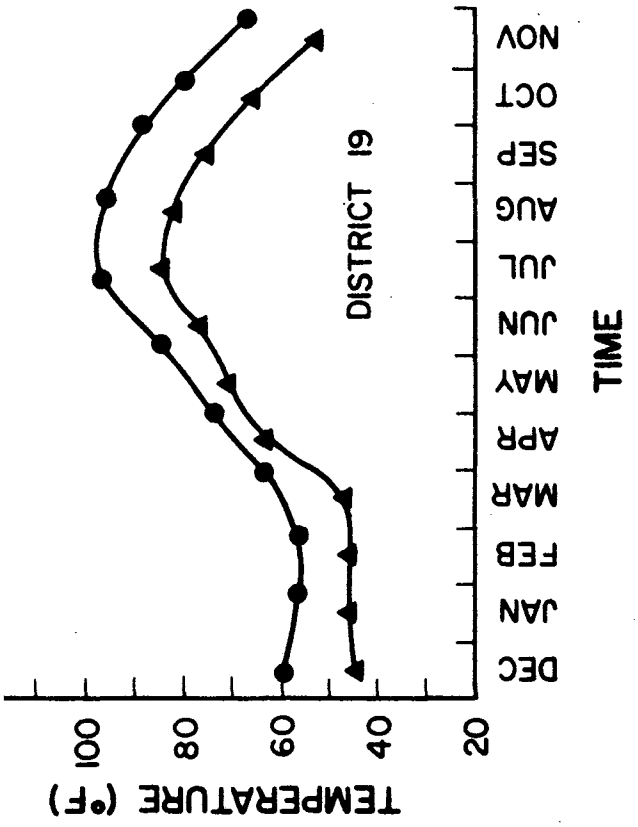
DISTRICT 19
TEMPERATURE (°F)
TIME
DEC
JAN
FEB
MAR
APR
MAY
JUN
JUL
AUG
SEP
OCT
NOV
20
40
60
80
100

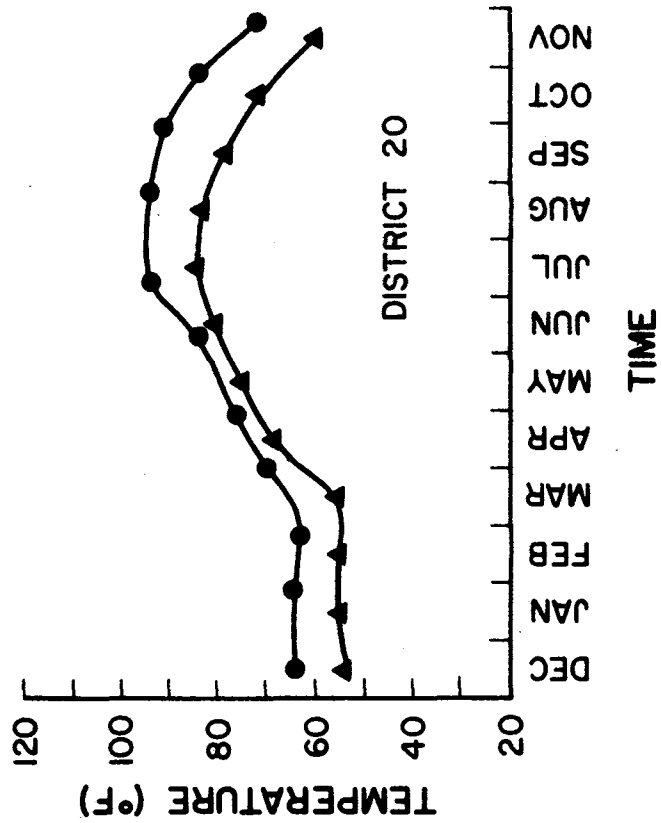
DISTRICT 20
TEMPERATURE (°F)
TIME
DEC
JAN
FEB
MAR
APR
MAY
JUN
JUL
AUG
SEP
OCT
NOV
20
40
60
80
100
120

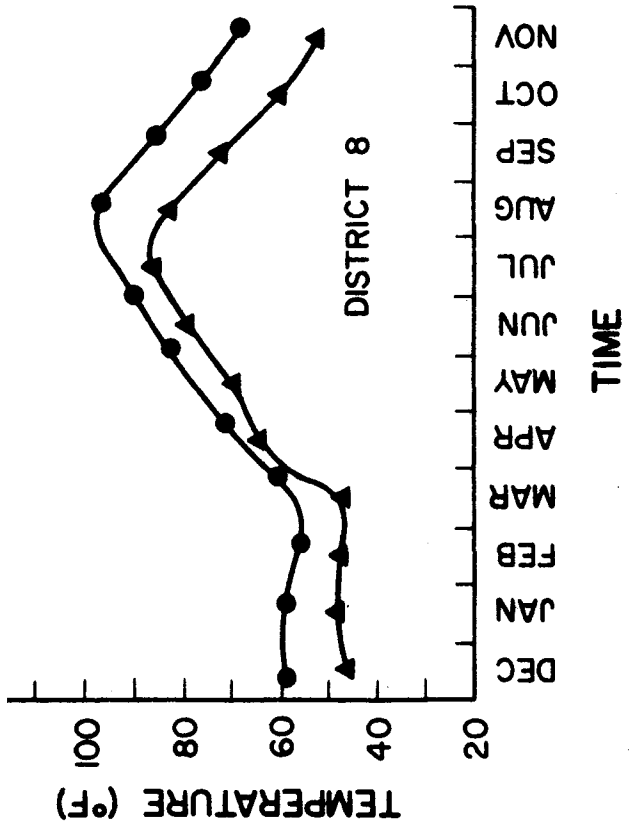
DISTRICT 8
TEMPERATURE (°F)
TIME
DEC
JAN
FEB
MAR
APR
MAY
JUN
JUL
AUG
SEP
OCT
NOV
20
40
60
80
100

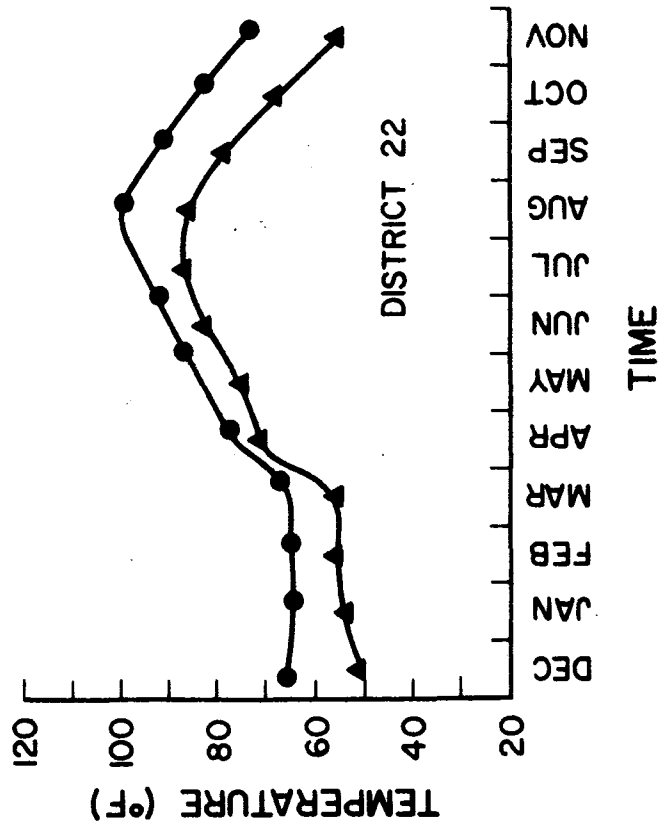
DISTRICT 22
TEMPERATURE (°F)
TIME
DEC
JAN
FEB
MAR
APR
MAY
JUN
JUL
AUG
SEP
OCT
NOV
20
40
60
80
100
120

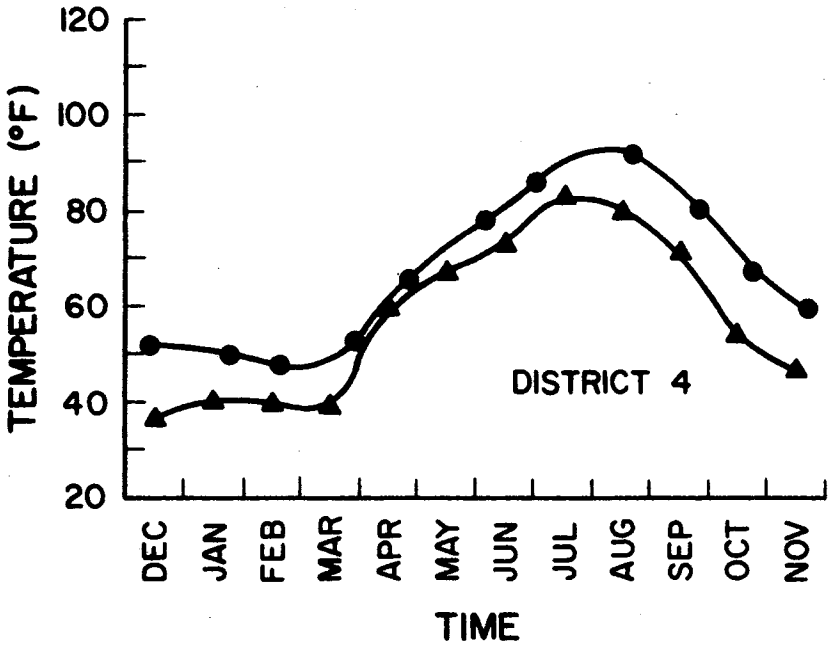

FIGURE 20b - Average monthly air and subgrade temperature versus time curves for District 4. Each subgrade data point is the average of 12 observations, one at each subsection. The air temperatures are from climatological data files. The circles are subgrade temperatures 36-inches below the surface and the triangles are air temperatures.

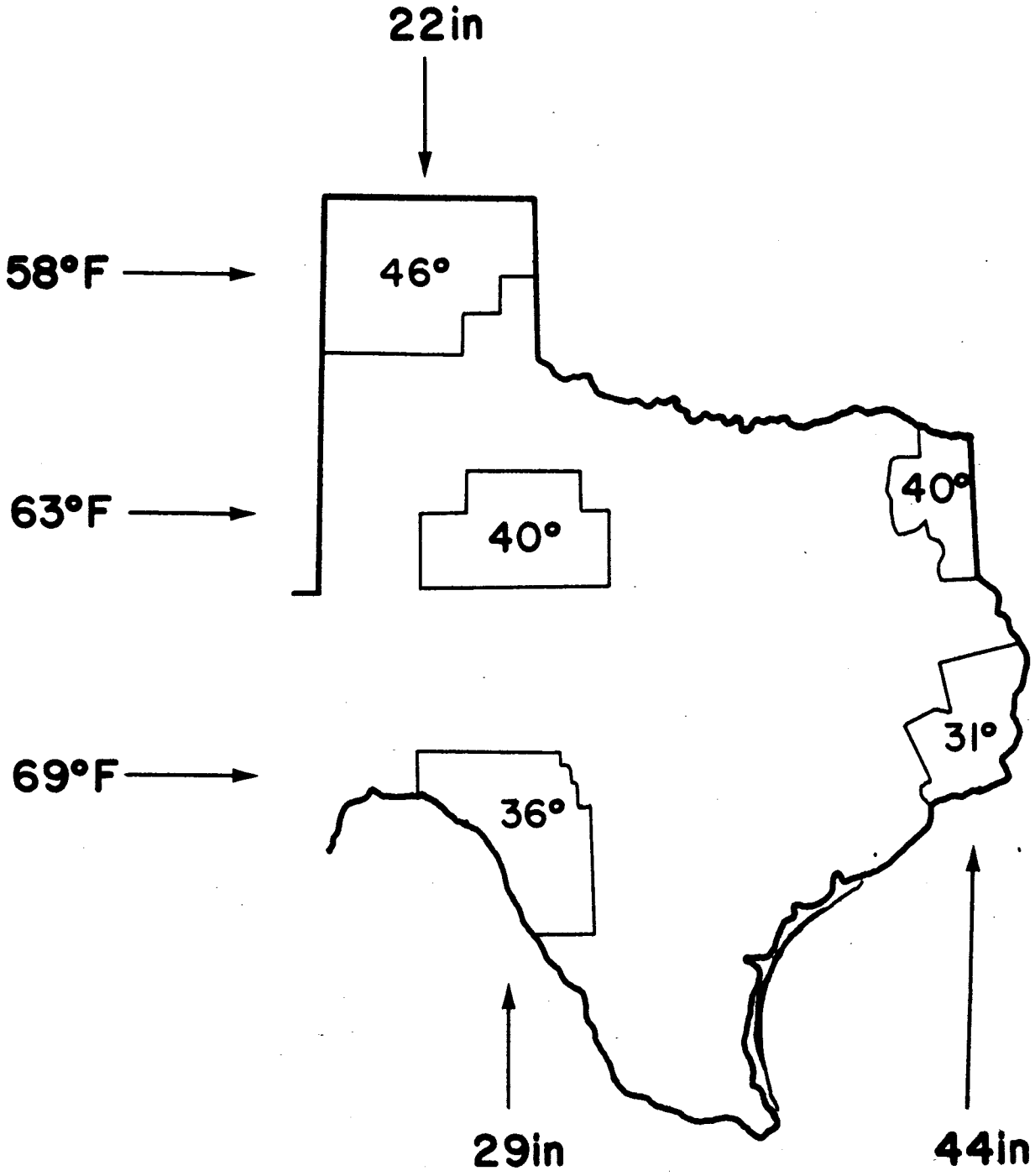

FIGURE 21 - The annual range of average monthly air temperatures for each district is shown on the map. The numbers outside the map represent average annual air temperature and total annual rainfall.

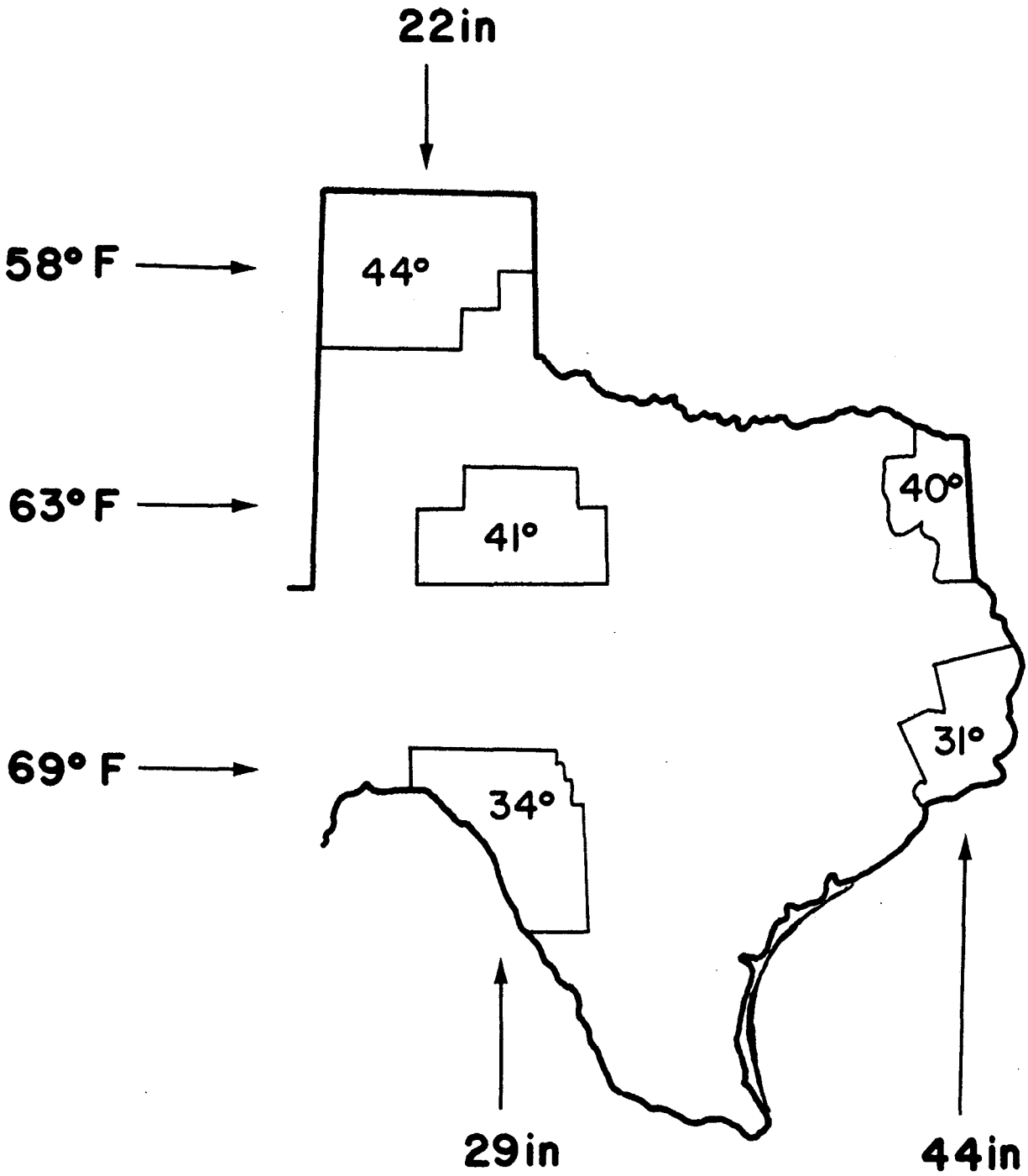

FIGURE 22 - The annual range of subgrade temperature for each district is shown on the map. The subgrade temperature was measured 36 inches below the surface at each subsection and averaged for the 12 subsections of each district. The numbers outside the map represent average annual air temperature and total annual rainfall.

Appendix C

Mechanical Analogy Used in Analysis of T-Data

This appendix refers to Section 4.4 of the main body of the report, and describes the method used in arriving at a mean or central value, $\tilde{T}$, of the times of occurrence, T, of the estimated annual maximum deflections at the 36 test points within a district.

Let T_i (where i = 1, 2, . . . , n) represent the ith value of T, which is defined as the time of occurrence of the maximum annual deflection at a given point in a district. The T-data is ordered as follows:

$$T_1 < T_2 < \ldots < T_{i-1} < T_i < T_{i+1} < \ldots < T_n.$$

Also, $0 \leq T \leq 365$, where T is zero at midnight, December 31.

A hypothetical set of T-data, with n = 4, has been plotted on the periphery of a circle in Figure 23 as an example of the mechanical analogy used to find T, the central value of the set. In this figure the circle, with a radius of unity, represents a disc or wheel mounted on a frictionless axle. The length of the circumference has been divided into 365 equal parts to represent the days in the year. Plotted as points on the periphery are the four values of T used in the example.

An origin of rectangular coordinates, x and y, is taken at the center of the disc. The coordinate system is fixed in space. Initially, the wheel is rotated on its axis until the zero point of the day scale (as well as the degree scale) is at the point x = 1 and y = 0, as shown in the lower right portion of Figure 23. Then a unit force vector, acting in the positive direction of the y-axis, is applied at each plotted point, and the wheel is released and allowed to come to rest

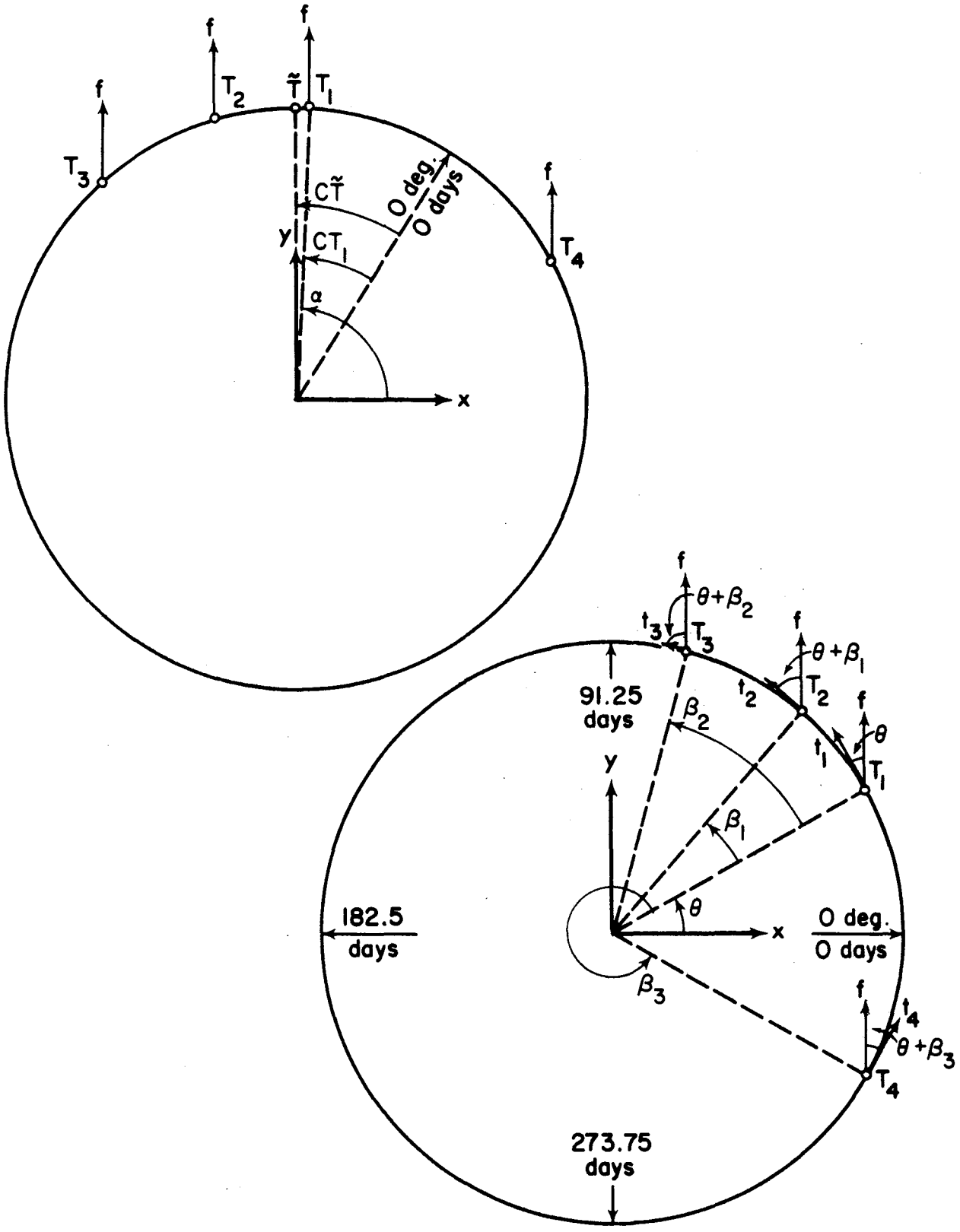

FIGURE 23 - Parameters for mechanical analogue used to find central value, $\bar{T}$, of T-data. Lower right: Unit forces act in y direction at each plotted value of T, tending to turn wheel. Upper left: Wheel at rest, with $\bar{T}$ on y-axis.

under the action of the unit forces, as illustrated at upper left in Figure 23.

At the moment of release, the angle θ, which defines the position in space of the point, T_1, at any instant, has the value, $360\ T_1/365$ degrees. The problem is to find the value of θ after the wheel has come to rest, and, from this value of θ, to find the central value, $\tilde{T}$.

Shown at lower right in Figure 23 are the torques, $t_1, t_2, \ldots, t_n$ tending to turn the wheel. These are related to the variable angle θ, and the constant angles $\beta_1, \beta_2, \ldots, \beta_{n-1}$ by the equations

$$t_1 = \cos \theta$$

$$t_2 = \cos (\theta + \beta_1)$$

$$t_3 = \cos (\theta + \beta_2)$$

$$\vdots$$

$$t_n = \cos (\theta + \beta_{n-1})$$

Values of the angles, β_i, in degrees, can be computed from the T-data by use of the following formulas:

$$\beta_1 = C(T_2 - T_1)$$

$$\beta_2 = C(T_3 - T_1)$$

$$\vdots$$

$$\beta_i = C(T_{i+1} - T_1)$$

$$\vdots$$

$$\beta_{n-1} = C(T_n - T_1)$$

where $C = 360/365$.

Let R be the net torque acting on the wheel. Then

$$R = \cos \theta + \cos (\theta + \beta_1) + \cos (\theta + \beta_2) + \ldots + \cos (\theta + \beta_{n-1}).$$

By making use of the trigonometric relationship

$$\cos(\theta + \beta) = \cos\theta \cos\beta - \sin\theta \sin\beta,$$

the equation for R can be written as

$$R = A_1 \cos\theta - A_2 \sin\theta, \tag{1}$$

where $A_1 = 1 + \cos\beta_1 + \cos\beta_2 + \ldots + \cos\beta_{n-1}$, (2)

and $A_2 = \sin\beta_1 + \sin\beta_2 + \ldots + \sin\beta_{n-1}$. (3)

After the wheel comes to rest, R = 0, or

$$A_1 \cos\theta - A_2 \sin\theta = 0.$$

There are two values of θ that satisfy this equation:

$$\theta_1 = \tan^{-1} \frac{A_1}{A_2}$$

and $$\theta_2 = \tan^{-1} \frac{A_1}{A_2} + 180°,$$

and only one of these values is desired, since the other represents an unstable condition. The choice between θ_1 and θ_2 can be made as follows:

Let α represent the value of θ when the wheel is in a stable condition, and let $\Delta\theta$, be a positive angle less than 180°. If $A_1 \cos(\theta_1 + \Delta\theta_1) - A_2 \sin(\theta_1 + \Delta\theta_1) < 0$, then $\alpha = \theta_1$; otherwise, $\alpha = \theta_2$.

The central value, $\tilde{T}$, corresponding to the angle, α, is then found as follows:

Let $k = (90° - \alpha + CT_1)/C$.

If $k \geq 0$, $\tilde{T} = k$; otherwise, $\tilde{T} = k + 365$.

Once the central value, $\tilde{T}$, is established, some measure of the density of the data in the vicinity of the central value is needed for comparing one set of data with another. Such a measure, referred to hereafter as the "grade," g, of the data, was developed as described below.

With the wheel at rest, let a small positive torque be applied to the wheel, displacing it through a small positive angle, $d\alpha$. A small negative reaction torque, dR_1, will result, as indicated by differentiating Equation 1:

$$dR_1 = -(A_1 \sin \alpha + A_2 \cos \alpha)\, d\alpha. \tag{4}$$

Now suppose that all the T-data are shifted (together with the unit force vectors) from their positions scattered around the rim of the wheel, and are concentrated at the point $T = \tilde{T}$. For this case the angles $\beta_1 = \beta_2 = \ldots = \beta_{n-1} = 0$, the constant $A_1 = n$ (according to Equation 2), the constant $A_2 = 0$ (according to Equation 3), and the angle $\alpha = 90°$. Again apply a small positive torque to the wheel, just sufficient to displace it through the same small positive angle, $d\alpha$, as before. The negative reaction, dR_2, found by making $A_1 = n$, $A_2 = 0$, and $\alpha = 90°$ in Equation 4, is $dR_2 = -nd\alpha$. (5)

The grade, g, is defined as the ratio, dR_1/dR_2; that is

$$g = \frac{dR_1}{dR_2}.$$

Thus, according to Equations 4 and 5,

$$g = \frac{A_1 \sin \alpha + A_2 \cos \alpha}{n}. \tag{6}$$

The maximum value of the grade, g, is 1.0, and could occur only if $T_1 = T_2 = \ldots = T_n$; that is, it could occur only if the maximum annual deflections at the 36 test points within the district all occurred on the same day. The minimum value of g is zero, and could occur only if the maximum annual deflections were evenly spaced throughout the year; in such an event, no central value of T would exist, since the "wheel" of the mechanical analogy could be brought to rest at any value of α.

The five sets of T-data analyzed in this study had grades ranging from 0.51 to 0.84. The grades, arranged in descending order, are given below, together with the corresponding values of $\tilde{T}$, and the identification of the source of the data in each case.

Source of Data (District)	Grade, g	Central Value, $\tilde{T}$	Corresponding Date
4	0.84	214.5	August 3
20	0.79	126.6	May 7
8	0.70	218.4	August 7
19	0.62	102.9	April 13
22	0.51	205.9	July 25

The grade, g, can be interpreted as a measure of the reliability of the central value, $\tilde{T}$.